DISCLAIMER NOTICE

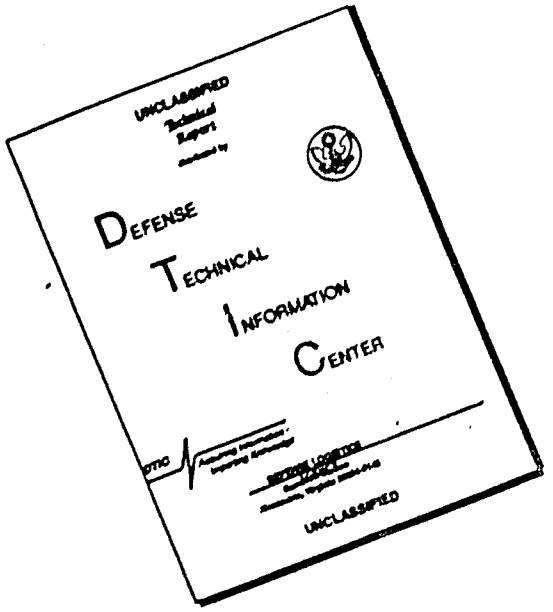

THIS DOCUMENT IS BEST QUALITY AVAILABLE. THE COPY FURNISHED TO DTIC CONTAINED A SIGNIFICANT NUMBER OF PAGES WHICH DO NOT REPRODUCE LEGIBLY.

COATINGS FOR SOLAR CELLS

Final Report

January 15, 1960 — February 28, 1961
Jet Propulsion Laboratory P. O. M-42848

Hoffman

Hoffman / ELECTRONICS CORPORATION

Santa Barbara, California

COATINGS FOR SOLAR CELLS

Final Report

January 15, 1960 — February 28, 1961
Jet Propulsion Laboratory P.O. M-42848

HOFFMAN SCIENCE CENTER
Hoffman Electronics Corporation
Post Office Drawer "H"
Santa Barbara, California

This report was prepared for the Jet Propulsion Laboratory, California Institute of Technology for use under NASA Contract NASw-6

Prepared By:

Robert M. Witucki
Arthur E. Lewis

Approved By:

Lloyd T. DeVore, Director
Hoffman Science Center

TABLE OF CONTENTS

Table of Contents - continued

LIST OF FIGURES

List of Figures - continued

List of Figures - continued

LIST OF TABLES

1 Introduction

About 9% of the total incident solar radiation in space is converted to electrical energy by Hoffman production-run silicon solar cells. However, more than 90% of the total solar radiation is absorbed by an uncoated cell. This excess energy absorbed is degraded to heat, which must be lost in space by re-radiation. An energy balance is therefore established for the cell, in which the radiation absorbed equals the electrical energy supplied to an external circuit plus the thermal energy radiated, and the cell attains an equilibrium temperature. Since in the temperature region of interest the conversion efficiency of solar cells increases as the temperature is decreased, it is important to achieve the lowest possible cell operating temperature. This can be done by rejecting unusable solar radiation by reflection, and by increasing the cell emissivity. Since uncoated cells absorb nearly all incident radiation, and since the cell surface has a very low emissivity, it becomes necessary to use cell coatings to accomplish these objectives.

The requirements of an ideal coating include a high reflectivity in the ultraviolet spectral region, high transmissivity in the visible to about 1.1 microns, high reflectivity just beyond the transmission cut-off, and high emissivity in the infrared beyond 4μ. In addition any coating to be used must be stable to all aspects of a space environment, including prolonged exposure to solar ultraviolet radiation and electron and proton bombardment.

The above requirements are presently being met in part by cementing very thin glass covers onto the front of the cell. Since the transparent cement used decreases in transmission from prolonged exposure to ultraviolet light, the cement must be protected. This is done by vacuum depositing on one side of the glass a 14-layer

interference type coating which selectively reflects ultraviolet radiation from about 0.3 to 0.45 microns. To increase absorption of the covered cell an antireflection coating is also deposited onto the front surface of the cover glass.

The objective of this contract was to increase cell efficiencies in space and to decrease the coating cost, by exploring possible coatings which would utilize optical properties of the coating material, rather than utilizing interference effects between multilayers.

2 Summary and Conclusions

The theoretical basis for the reflectance of dielectric materials in the ultraviolet and the near infrared has been reviewed, as well as the properties required for high emissivity. From these considerations it was concluded that single thin film coatings alone, of 1 micron or less in thickness, can not provide either adequate emissivity or high selective reflectivity of the wavelengths required and still show high transmission from 0.45 to 1.1 microns. A high emissivity was found to be the most important single method of rejecting energy in space. Therefore attention was directed primarily toward achieving maximum emissivity. Emissivities of the order of 0.9 can only be obtained using coatings of several mils thickness.

Silicone coatings were found to be very simple and inexpensive to apply, and within the accuracy of available data to show a predicted performance in space equivalent to the presently used ultraviolet reflecting coated cover glasses. Numerous laboratory tests of limited time duration have shown the selected silicone coating to be stable to the expected environmental conditions during storage as well as in space. However, the stability of the coating to prolonged ultraviolet solar radiation in space must still be established

One sample of the silicone coating selected has successfully withstood exposure to ultraviolet radiation, in an argon atmosphere, for an estimated 20 equivalent sun days in space. However, the coatings rapidly degrade under ultraviolet radiation in the presence of any reactive impurities in the atmosphere. Detailed ultraviolet tests of longer duration will be required, with spectrally defined ultraviolet radiation and with the atmospheric purity and coating temperature rigorously controlled in order to experimentally determine lifetimes in space environment.

3 Effect of Coatings on Solar Cell Conversion Efficiency in Space

In order to establish the optimum coating characteristics, equilibrium solar cell temperatures have been calculated for various cut-off points from high reflectivity to high transmissivity in both the ultraviolet and infrared, as well as for the cross-over point from high reflectivity to high emissivity in the infrared. All of these calculations are based on the solar spectrum given by Johnson, (1) reproduced in Fig. 1, which is for zero air mass, and all cell efficiencies considered subsequently are based on this curve. Calculations were made graphically with the use of a planimeter, together with a radiation calculator slide rule. Solar cells of 9% conversion efficiency in space are used for these calculations. (This corresponds to a conversion efficiency of 12% as measured conventionally using a tungsten source.)

3.1 Calculated Cell Temperatures with Coatings of Various Assumed Optical Properties

The energy in various portions of the solar spectrum and the electrical energy produced by a cell with 9% efficiency in space are shown in Fig. 2. The energy conversion curve for the cell was calculated using the spectral response curve given in reference 2. These values were then used to calculate the results shown in Table I. On the basis of these preliminary calculations, the desired properties of a coating in order of importance are:

1. High transparency from 0.4 to 1.1μ;
2. High emissivity above 4μ;
3. High reflectivity from 1.1 to 4μ;
4. High reflectivity below 0.4μ.

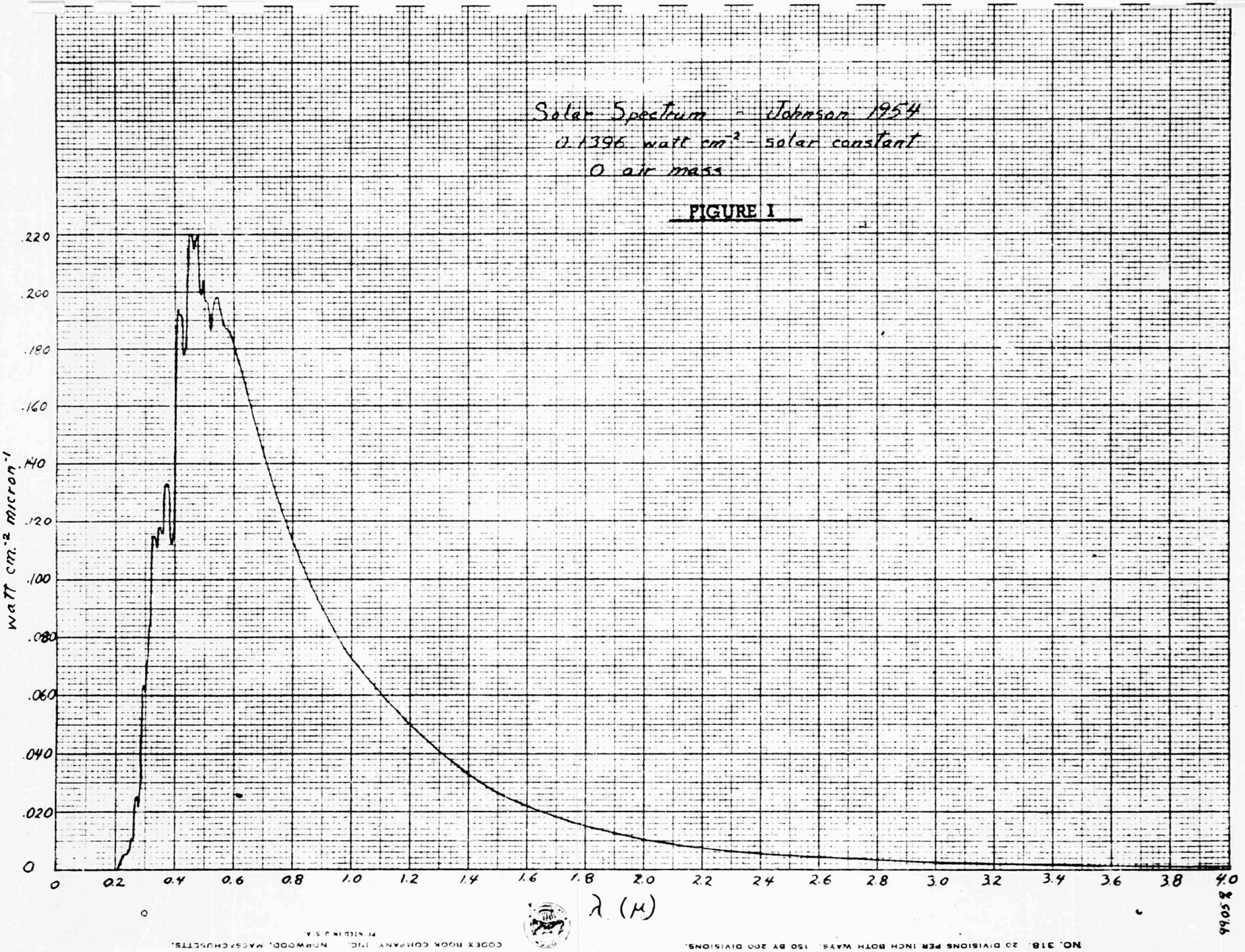

FIGURE I

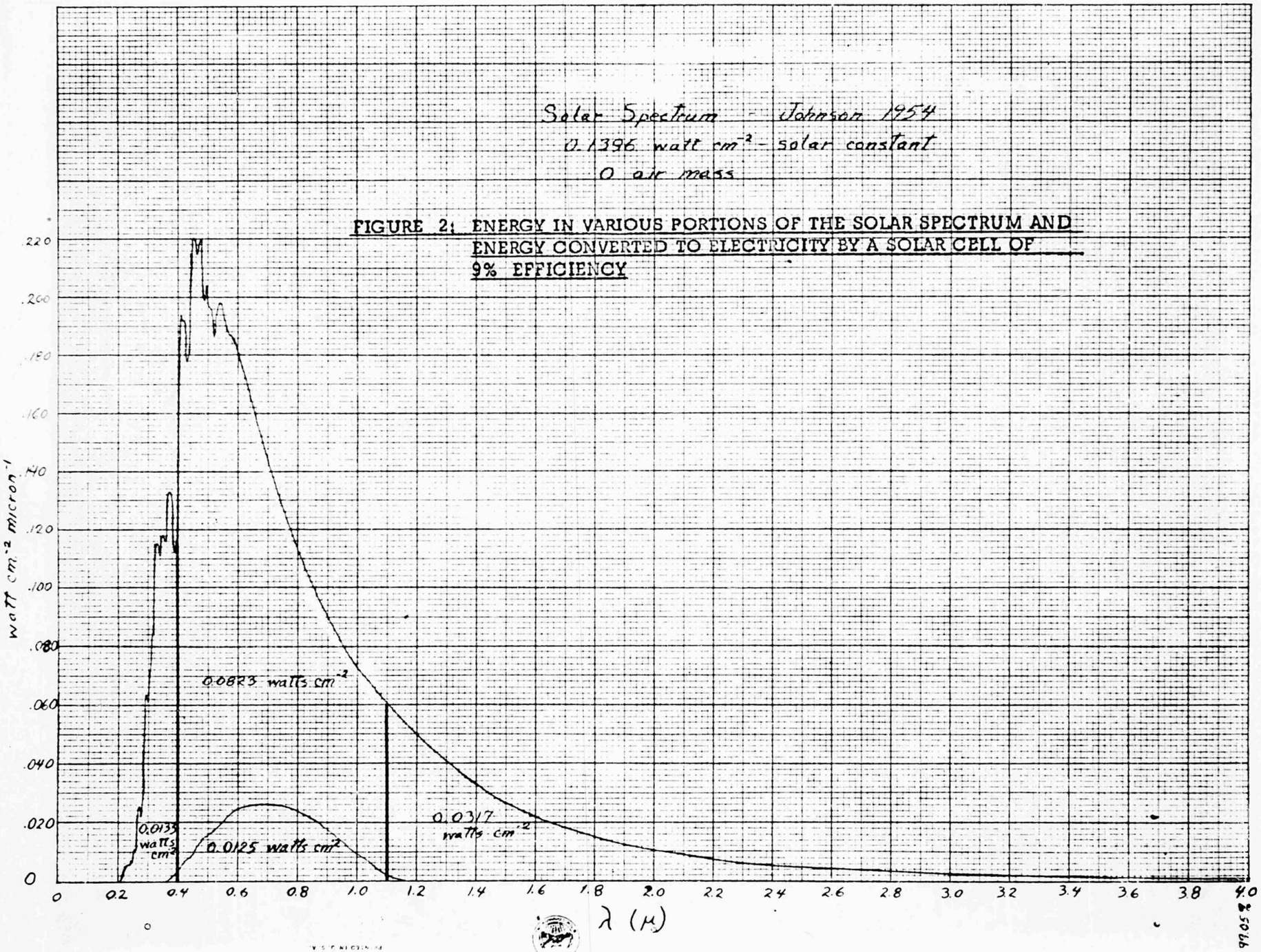

FIGURE 2: ENERGY IN VARIOUS PORTIONS OF THE SOLAR SPECTRUM AND ENERGY CONVERTED TO ELECTRICITY BY A SOLAR CELL OF 9% EFFICIENCY

TABLE I: CELL OPERATING TEMPERATURES & CONVERSION EFFICIENCIES

	Emissivity of Front Surface of Cell				
	0	.25	.50	.75	1.0
A = 1 (0 - 4μ)	119°C 4.9%	98°C 5.8%	80°C 6.6%	64°C 7.2%	53°C 7.7%
A = 1(.4 - 4μ) R = 1(0 - .4μ)	108°C 5.4%	87°C 6.3%	69°C 7.0%	56°C 7.6%	45°C 8.1%
A = 1(0 - 1.1μ) R = 1(1.1 - 4μ)	93°C 6.0%	73°C 7.0%	56°C 7.6%	42°C 8.2%	32°C 8.7%
A = 1(.4 - 1.1μ) R = 1(0 - .4μ) R = 1(1.1 - 4μ)	80°C 6.6%	61°C 7.5%	45°C 8.1%	32°C 8.7%	22°C 9.1%

A = Absorptivity
R = Reflectivity

Assumptions:

Cell efficiency in space is 9% at 25°C.

Solar Constant = 0.1396 watts/cm^2.

Energy is radiated from both the front and rear surfaces of the cell, assuming an emissivity of unity for the rear surface.

Cell efficiencies at various temperatures are calculated using temperature dependence data from Ref. 2 assuming a load matched at the calculated temperature.

The wavelength values listed here are approximate; more exact cut-off and cross-over points are calculated in following parts of this report. However, using the optimum cut-off points obtained subsequently, the minimum cell operating temperature is calculated to be 8^{o}C. (Fig. 3), as compared to 22^{o}C. in Table I.

3.2 Spectral Response and Solar Response of 9% Cell

The solar spectrum and the relative cell response at constant light intensity are plotted in Fig. 4, using arbitrary energy units for relative cell response. The relative cell response curve was determined using a tungsten light source, the dashed portion being extrapolated.

The product of these curves gives the relative cell response to solar radiation, also plotted using arbitrary energy units. The area labeled electrical energy is proportional to the relative cell response for the solar spectrum, and equals 9% of the total area under the solar spectral curve, or 0.01255 watts/cm.^{2}

3.3 Optimum Transmission Cut-Offs for Cell Coatings

The optimum transmission cut-offs, or the limits of useful radiation for a cell operating in vacuum, include the spectral band that results in the maximum power output of a solar cell. As either transmission cut-off is shifted in either direction the power output decreases. The factors that determine these cut-offs include: the change in cell output as a function of temperature, the conversion efficiency of a cell as a function of the wavelength of incident radiation, and the emissivity of both the front and back surfaces of the cell.

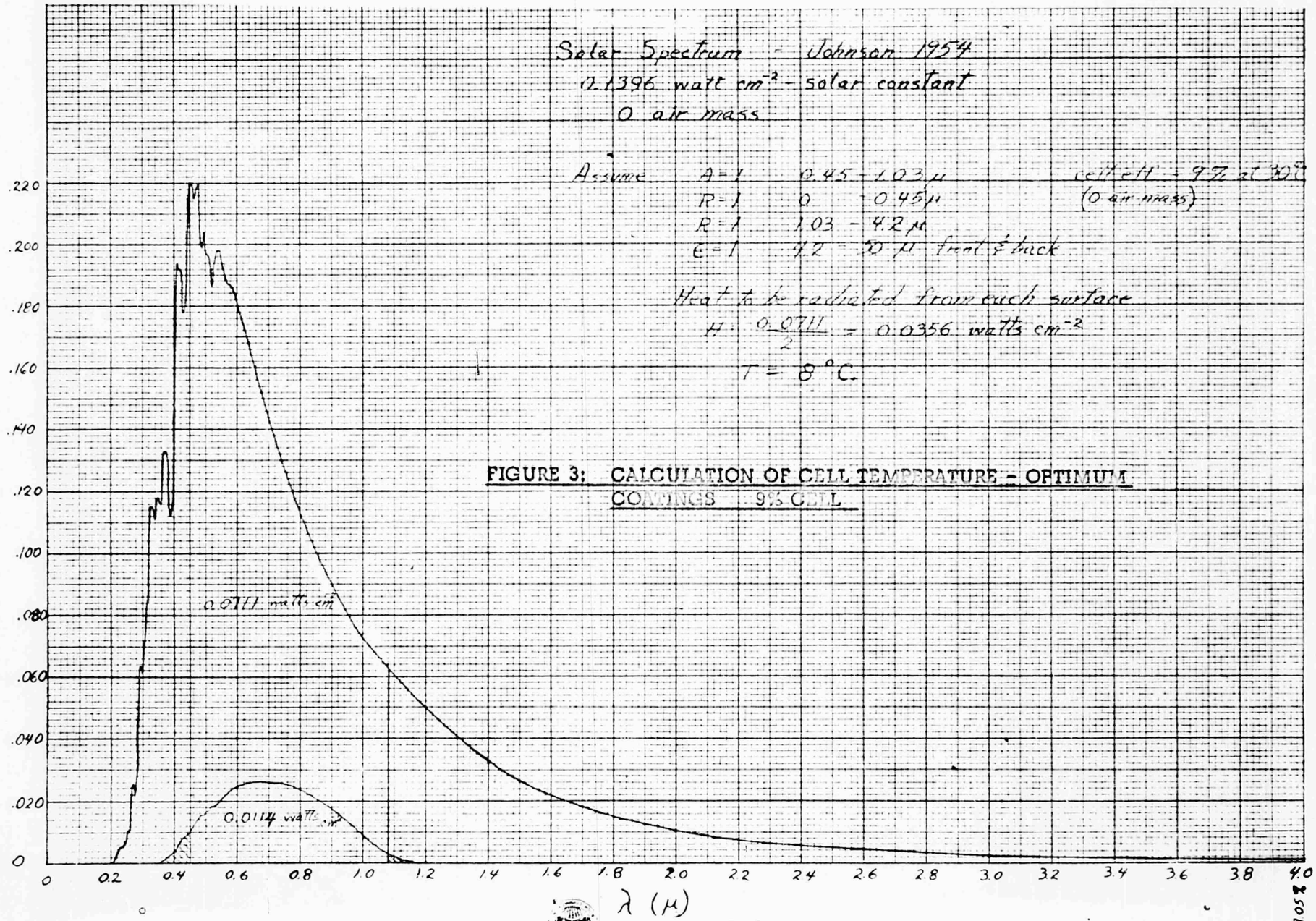

FIGURE 3: CALCULATION OF CELL TEMPERATURE - OPTIMUM COATINGS - 9% CELL

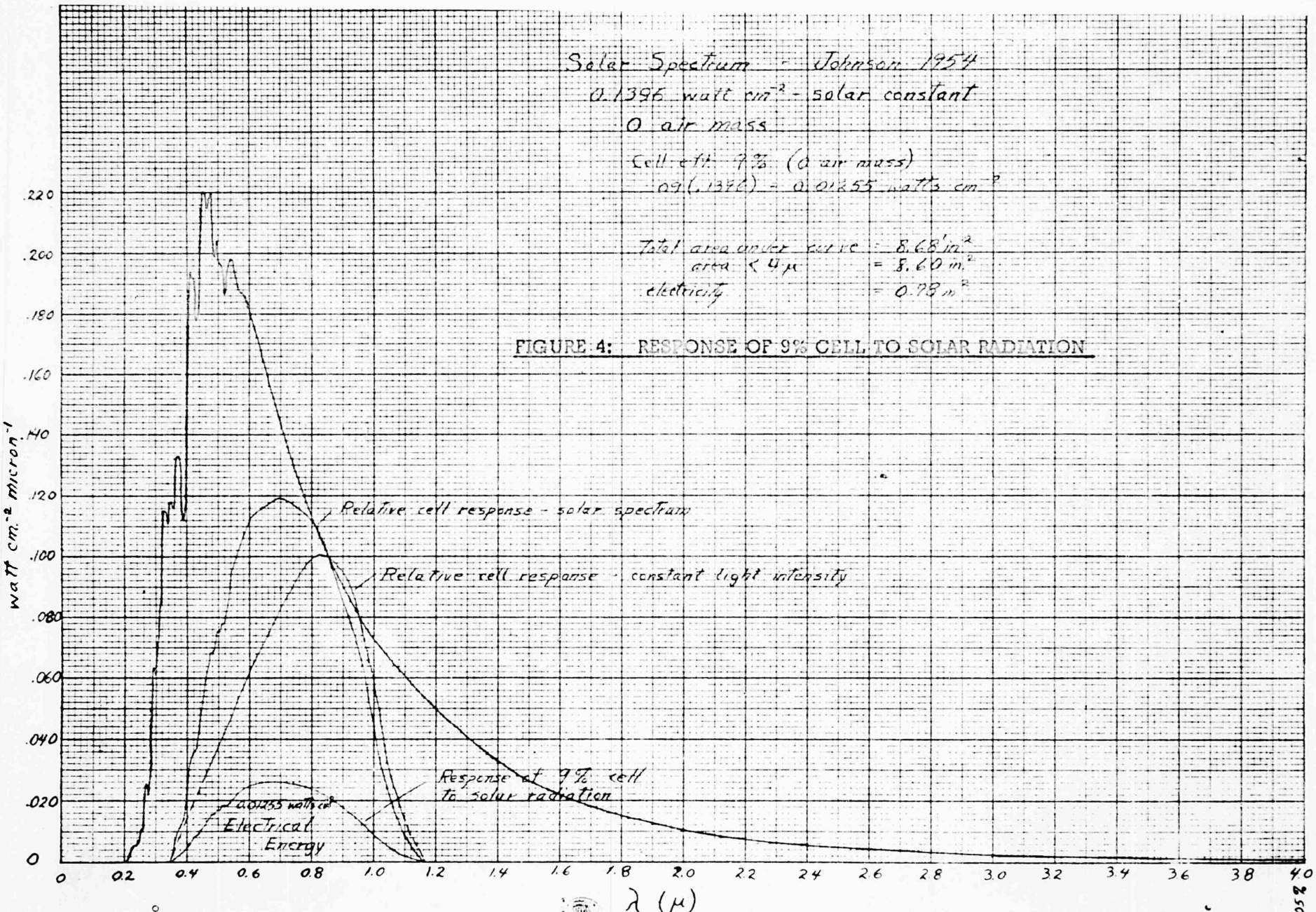

FIGURE 4: RESPONSE OF 9% CELL TO SOLAR RADIATION

The maximum power output of a cell at various temperatures, as compared to the maximum output of a cell at $30^{\circ}C.$, is given in Fig. 5. The spectral conversion efficiency of a 9% cell is shown in Fig. 6, together with the optimum cutoff points for three values of emissivity.

The most important variable affecting the equilibrium operating temperature in space is the emissivity of the cell. Emissivity calculations have been made using the Stefan-Boltzmann law, assuming that the spectral distribution of radiation from the cell surface is directly proportional to a black body distribution. A sample of calculations used to plot Fig. 6 is given below.

From the Stefan-Boltzmann law a black body at $30^{\circ}C.$ radiates 0.000628 watts/$cm.^2$ more than a body at $29^{\circ}C.$ At equilibrium in a vacuum, the body receives as much radiation as it radiates. If one surface receives and two are free to radiate as is the case with a solar cell, then the energy the cell receives on one surface may be twice as large, or 0.001256 watts $cm.^{-2}$, for the same temperature change of $1^{\circ}C.$

The loss of efficiency resulting from a $1^{\circ}C.$ temperature rise is 0.486% from $30^{\circ}C.$ to approximately $110^{\circ}C.$ (see Fig. 4). Below $30^{\circ}C.$, the efficiency loss is smaller. The loss of electrical energy at $30^{\circ}C.$ for a 1° temperature rise in a 9% efficient cell is

$$\Delta W_e = (.09)\ (.1396)\ (.00486) = 0.0000610 \text{ watts cm.}^{-2}.$$

The radiation received must make enough electricity to compensate for the loss in output due to the temperature rise. The total radiation absorbed, W, is converted to heat, W_h, or to

FIGURE 5: CELL OUTPUT VERSUS TEMPERATURE

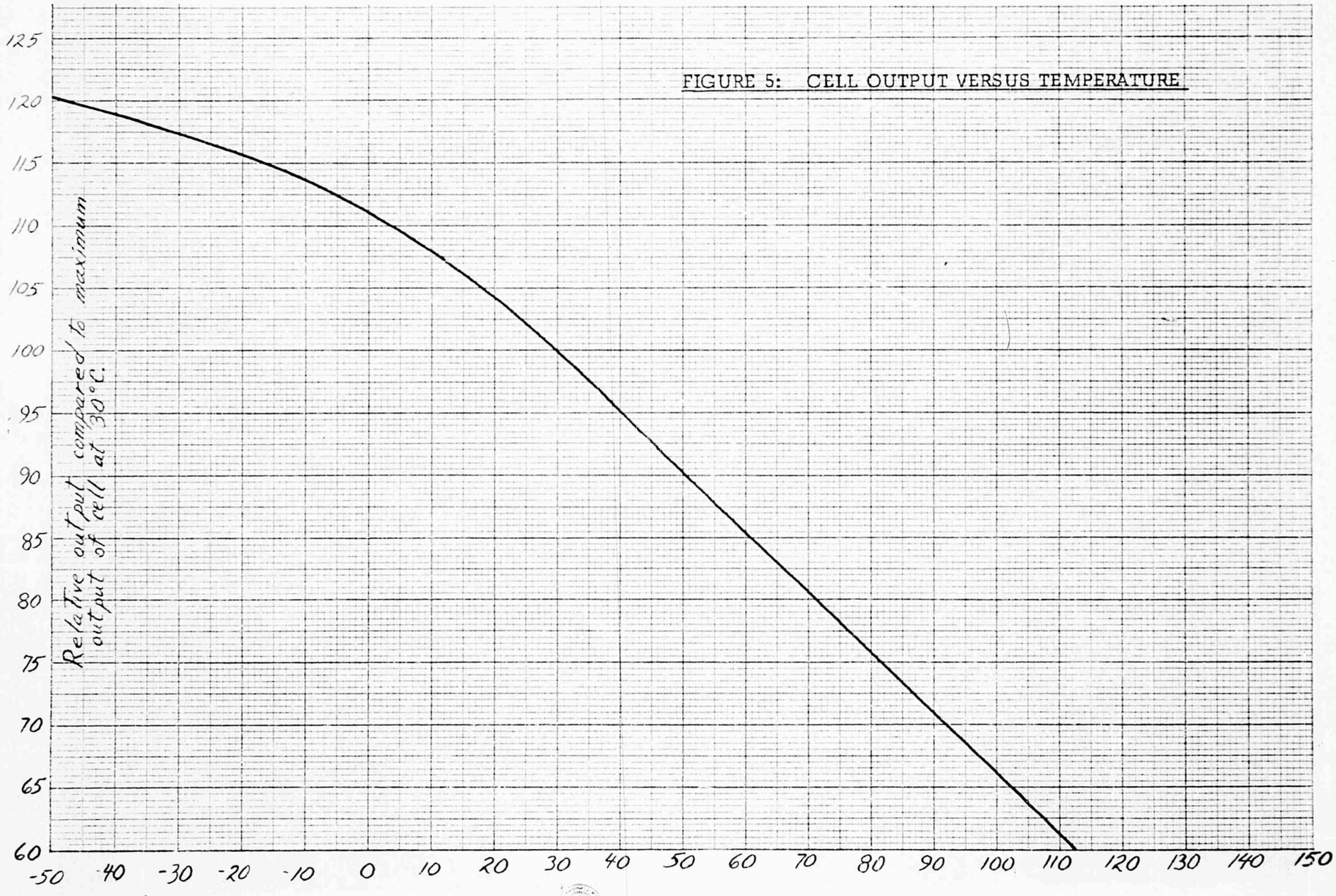

FIGURE 6:

Spectral response of solar cells and minimum useful conversion efficiency for 1 To cell (0 air mass) for various total emissivities tungsten source - constant light intensity

$$\epsilon = \frac{\epsilon_{front} + \epsilon_{back}}{2}$$

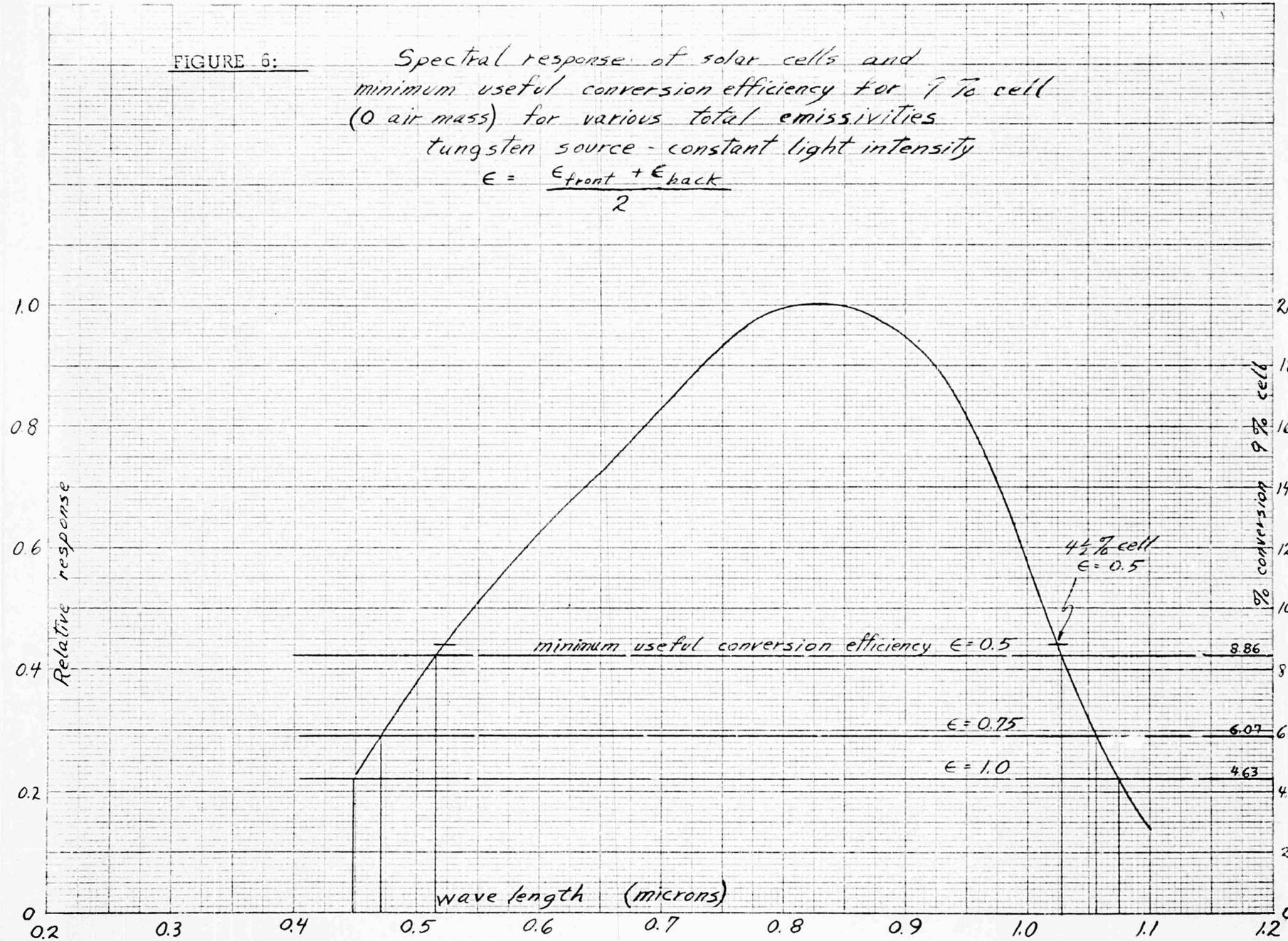

electricity, W_e. For a cell with emissivity of 1 on each radiating surface, or a total emissivity of 1,

$$W = W_h + W_e$$

$$W = 0.001256 + 0.0000610 = 0.001317 \text{ watts cm}^{-2},$$

and the minimum useful conversion efficiency is

$$\frac{W_e}{W} = \frac{0.000061}{0.001317} = 0.0463 \text{ or } 4.63\%.$$

The results of similar calculations for other emissivities are given in Fig. 6.

The intersections of the minimum useful conversion efficiency lines and the per cent conversion versus wavelength curve yield cut-off points for the useful radiation range. The cut-off points for a 9% cell are shown in Fig. 6. For $\epsilon = 0.5$, the useful range is 0.515μ to 1.03μ. For $\epsilon = 0.75$, the useful range is 0.47μ to 1.06μ. For $\epsilon = 1.0$, the useful range is 0.45μ to 1.08μ.

The cut-off points do not change much for cells of different efficiency. For a 4-1/2% cell, and $\epsilon = 0.5$

$$W = 0.000628 + 0.0000305 = 0.0006585$$

and the minimum useful conversion efficiency is

$$\frac{W_e}{W_h} = \frac{0.0000305}{0.0006585} = 0.0463 \text{ or } 4.73\%.$$

This point is shown on Fig. 6 for comparison with the 9% cell; however, it should be noted that the ordinate scale for a 4-1/2% cell is not the same as for a 9% cell.

3.4 Optimum Cross-Over Point in the Infrared from High Reflectivity to High Emissivity

The spectral distribution of sunlight, together with curves showing the energy radiated from two sides of a thin sheet black body at several temperatures, are given in Fig. 7. These latter curves are black body curves with the ordinates multiplied by two, or black body x 2 curves. The intersection of the solar spectrum and the black body x 2 spectrum for any temperature is the cross-over point for that temperature.

If the total emissivity $(\frac{\epsilon \text{ front} + \epsilon \text{ back}}{2})$ is less than 1, then a proportional part of the black body x 2 curve must be used to determine the cross-over wavelength. For example, if the total emissivity is 0.5 and the temperature is 100°C., the intersection will be at 3.58μ instead of 3.33μ. The optimum cross-over point in the infrared from high reflectivity to high emissivity is plotted in Fig. 8 as a function of temperature for various total emissivities. Fig. 8 is derived directly from Fig. 7.

The exact location of this cross-over point in the infrared is not as important as the transmission cut-offs considered previously. At 30°C., the cross-over wavelength may vary between 3.1μ and 5.4μ, and the cell temperature will remain within 1°C. of the temperature at the optimum cross-over point, 4.2μ. These numbers were calculated from Fig. 7. The area under each curve is proportional to the energy in each wavelength range. The area under the solar spectrum between 3μ and 5μ was measured as 2.86 in.^{2}, and the energy is .0161(.1396) = 0.002247 watts cm.$^{-2}$ in this range.

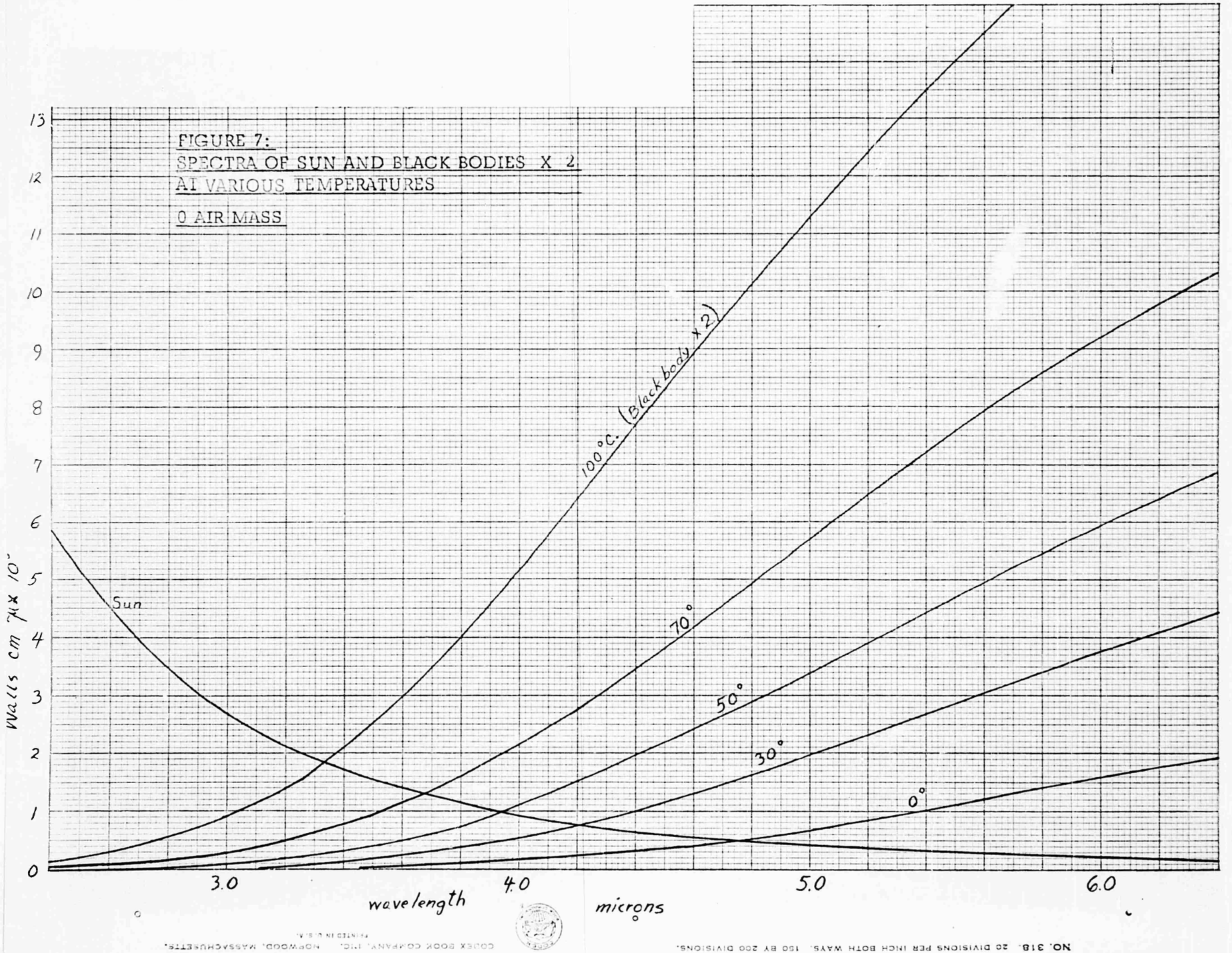

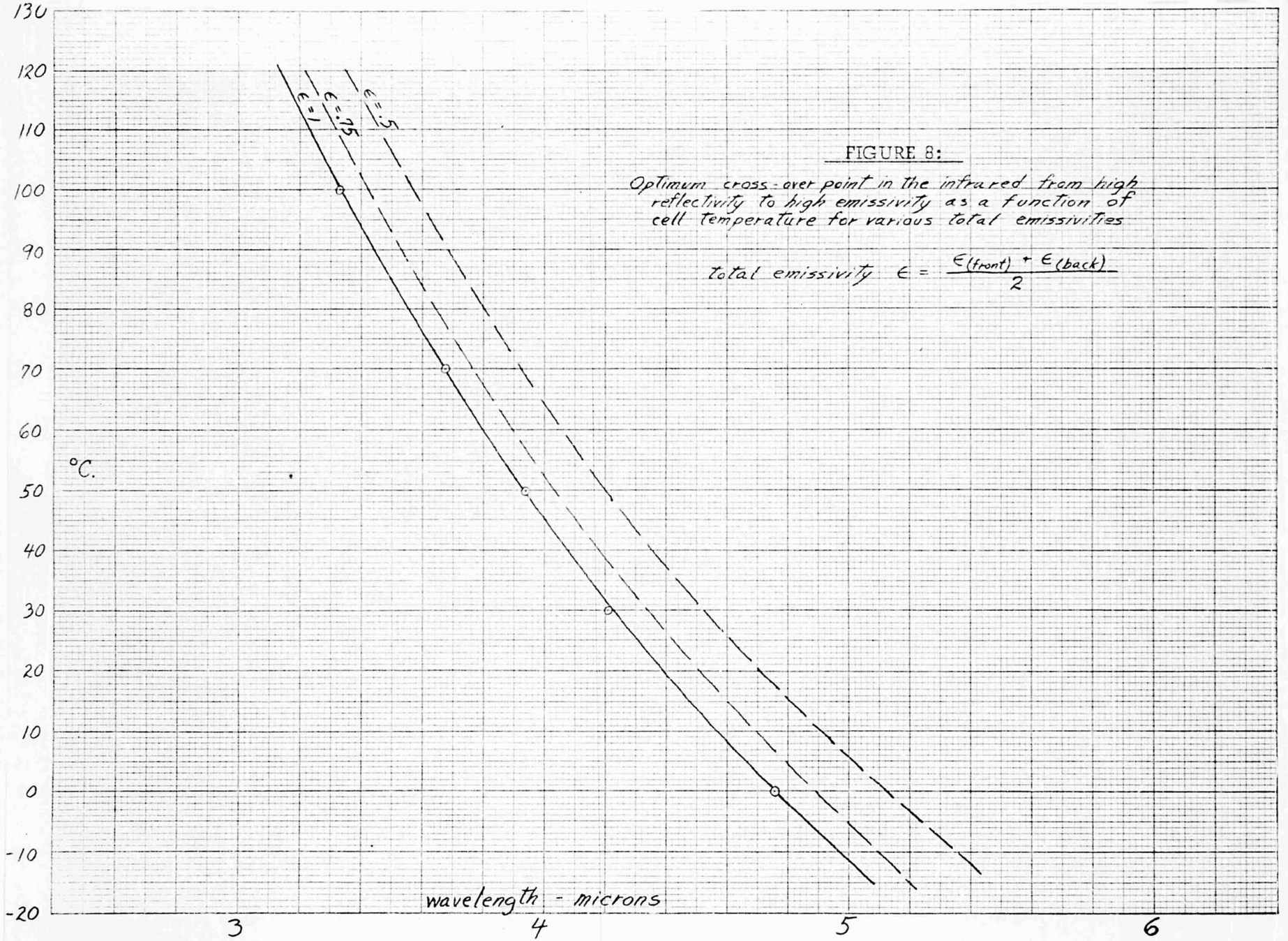

FIGURE 8:

Optimum cross-over point in the infrared from high reflectivity to high emissivity as a function of cell temperature for various total emissivities

total emissivity $\epsilon = \frac{\epsilon_{(front)} + \epsilon_{(back)}}{2}$

As determined earlier, 0.000628 watts $cm.^{-2}$ of energy is required for a temperature change of $1^{\circ}C.$ at $30^{\circ}C.$ if $\epsilon = 0.5$, and 0.001256 watts $cm.^{-2}$ if $\epsilon = 1$.

For $\epsilon = 1$

$$\frac{x(in.)^2}{2.86\ in.^2} = \frac{0.001256\ watts\ cm.^{-2}}{0.002247\ watts\ cm.^{-2}}$$

$$x = 1.57\ in.^2.$$

The area between the solar radiation curve and the black body x 2 curve in Fig. 6 must therefore equal $1.57 in.^2$ before the temperature is raised or lowered $1^{\circ}C.$

4 Theoretical Basis for the Reflectivity and Emissivity of Dielectric Materials

The objective of this work was to develop a coating for solar cells, with optical properties dependent primarily on material properties rather than interference phenomena, which in greatest degree meets the following specifications: The coating should have a reflectivity of unity in the ultraviolet to about 0.46 microns, a transmissivity of unity from this point to about 1.1 microns, a reflectivity of unity from this point to about 4 microns, and an emissivity of unity from this point to about 40 microns. The locations and relative importance of these cut-off points are discussed in detail in the first section of this report.

In order to approach this problem systematically, rather than simply evaluating a large number of materials, it is necessary to consider the theoretical bases for the desired properties and to use these as guides in selecting materials for evaluation. This approach will also provide an insight into whether or not it will be possible to achieve the total objective as summarized above by utilizing only material properties.

4.1 Transmissivity

Any coating used must have a high transmission from about 0.46 microns to about 1.1 microns. This requirement limits possible coating materials to dielectrics and to semiconducting materials having no absorption band in the desired transmission range. In addition, in order to keep front surface reflection losses to a minimum, the materials should have a low index of refraction.

4.2 Reflectivity

In classical electromagnetic theory high absorptivity, high reflectivity, and anomalous dispersion are associated with the natural frequencies of oscillators in any material. A schematic diagram of the complete dispersion curve for a dielectric material is shown in Fig. 9, the dashed lines showing regions of anomalous dispersion. Each region of anomalous dispersion is associated with an absorption band and an oscillator in the material. The absorption bands in the X-ray spectral region arise from the natural frequency of oscillation of the innermost electrons in the atoms; the absorption band in the ultraviolet from valence electrons in molecules and crystals; the absorption band in the near infrared from the oscillation of bound atoms in molecules or crystals; and the absorption bands in the far infrared and microwave regions from lower frequency oscillations arising from vibrational, rotational, and other complex modes in the molecules and crystals. The absorption bands in the ultraviolet and in the infrared are of interest here as they relate to the reflectivity of materials in these spectral ranges, and to the emissivity in the infrared.

In regions of strong absorption, materials are opaque, and any incident radiation is partially reflected and partially absorbed. The relationship between these two effects depends on the nature of the oscillator responsible for the absorption. Specifically, if the oscillator vibrates with little or no dissipation of energy, then strong reflection will result. Therefore, for the reflectivity properties of coatings desired in this work, it will be essential to find materials which have strong absorption bands, with oscillators of the right type, in the desired spectral regions.

FIGURE 9: SCHEMATIC DISPERSION CURVE FOR A DIELECTRIC MATERIAL

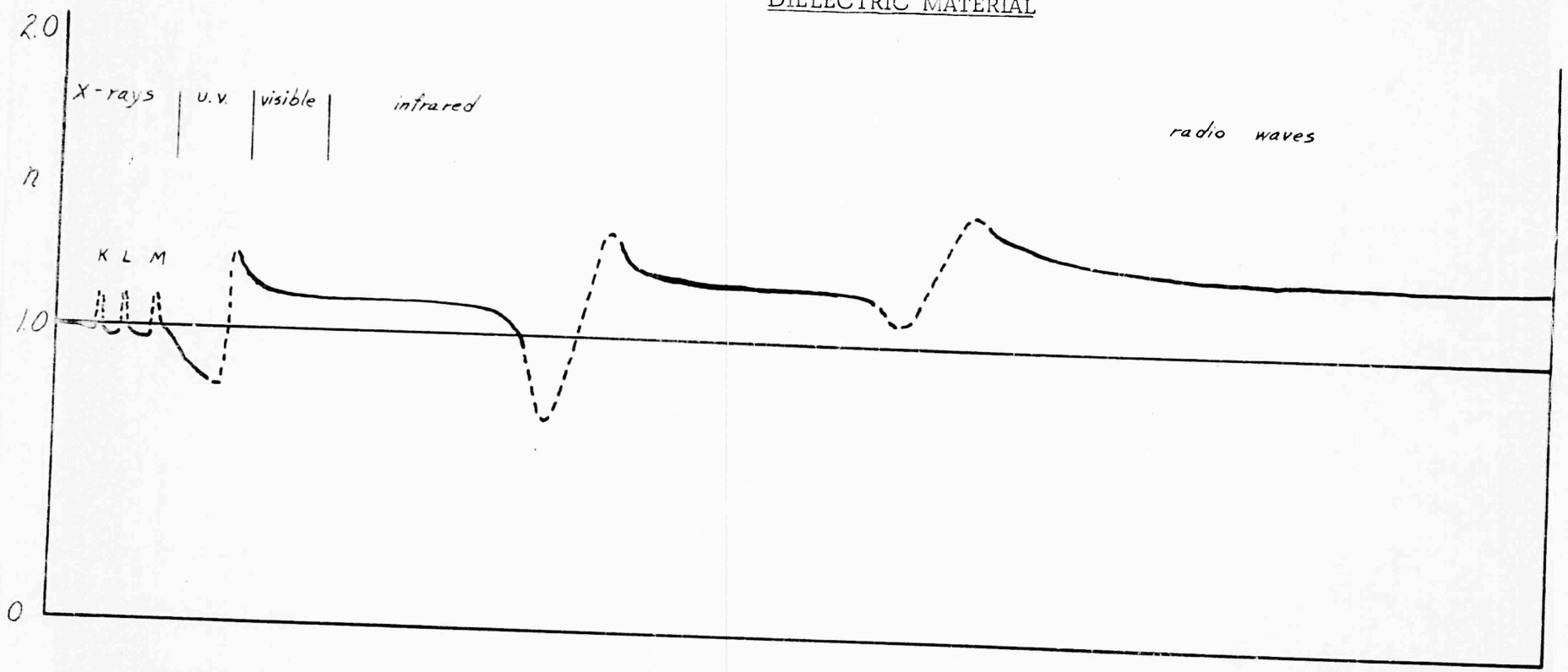

4.2.1 Infrared Reflectivity

The reflectivity of dielectric materials in the spectral region from 1 to 15 microns results from molecular or structural vibrations, rather than from electronic vibrations as in the ultraviolet. A general idea of the requirements for a material to reflect in the infrared can be obtained by considering a model of a diatomic molecule. The frequency of such an oscillator can be represented by

$$\nu = \frac{1}{2\pi c}\sqrt{\frac{f}{\mu}}$$

where ν is the wave number in $cm.^{-1}$, c is the velocity of light, f is the force constant of the bond, and μ is the reduced mass of the molecule, given by $\frac{1}{\mu} = \frac{1}{\mu_1} + \frac{1}{\mu_2}$. This relation shows that the frequency of oscillation, and therefore the frequency of radiation absorbed, is proportional to the square root of the force constant of the bond, and inversely proportional to the square root of the reduced mass. Therefore the shortest wavelengths that will be absorbed will be for oscillators having the lowest reduced mass and the greatest force constants.

A general survey of the absorption spectra of materials shows that absorption related to structural vibrational modes generally occurs for wavelengths greater than about 10 microns. For example, fused silica has strong absorption and related high reflectivity at about 8.5 microns. In this case the silicon-oxygen bond is responsible for the high reflectivity. Materials with absorption bands at shorter wavelengths include a number of hydrogen compounds such as water, many hydrides in which the small mass of the hydrogen is responsible, and compounds such as carbon dioxide and various metal carbonates in which both the relatively small masses of the carbon

and oxygen and the large force constant of the carbon-oxygen bond are important. From the materials surveyed to date there appears to be no possibility of finding a coating material which will have a high selective reflectivity in the region of 1 - 2 microns, and which will have the physical properties required for the proposed application.

4.2.2 Ultraviolet Reflectivity

The normal reflectivity (R) of a material is related to the index of refraction, n, and to the extinction coefficient, k_o, by the expression

$$R = \frac{(n-1)^2 + k_o^2}{(n+1)^2 + k_o^2}$$

Fig. 10 shows this relationship graphically for a theoretical material, while Fig. 11 shows a plot of the reflectivity for various values of n and k_o. Therefore, given dispersion data and absorption data for any material, it is possible to calculate the normal reflectivity.

Any material having a selective reflectance in the near ultraviolet has an absorption band in the region of the desired reflectance. Since the index of refraction varies rapidly in the region of an absorption band it is therefore possible to make an initial selection of possible reflecting materials of interest either on the basis of dispersion data or of absorption data.

One characteristic of semiconducting materials is that they show an optical absorption edge determined by their band gap. The absorption edge is defined as the point where the slope of the absorption coefficient is a maximum. the absorption coefficient, α, being related to the extinction coefficient, k_o, by

$$k_o = \alpha\lambda/4\pi.$$

FIGURE 10: RELATIONSHIP OF REFLECTIVITY TO THE OPTICAL CONSTANTS n AND k_o FOR A THEORETICAL MATERIAL NEAR AN ABSORPTION BAND

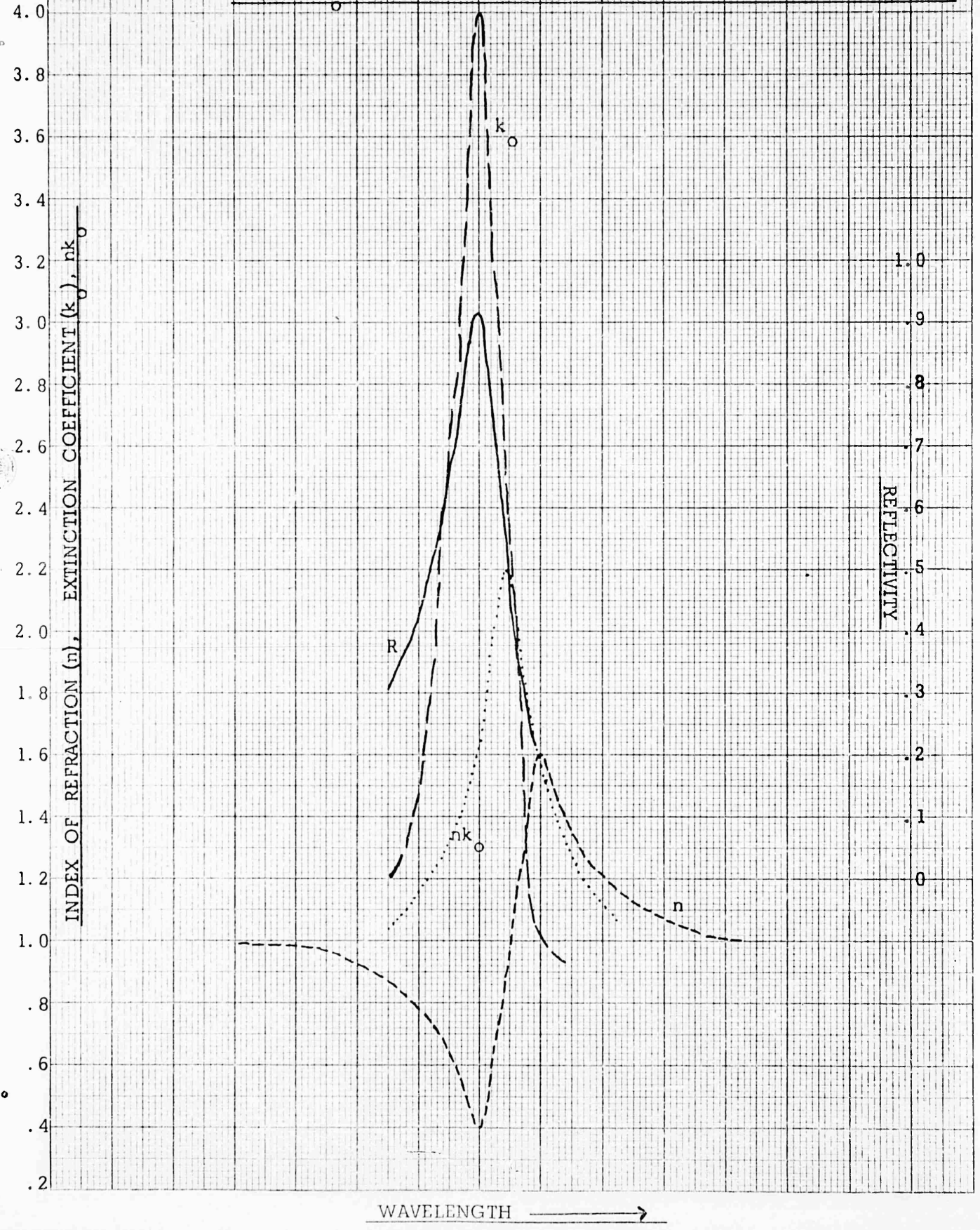

FIGURE 11.

REFLECTIVITY AS A FUNCTION OF n AND k_o

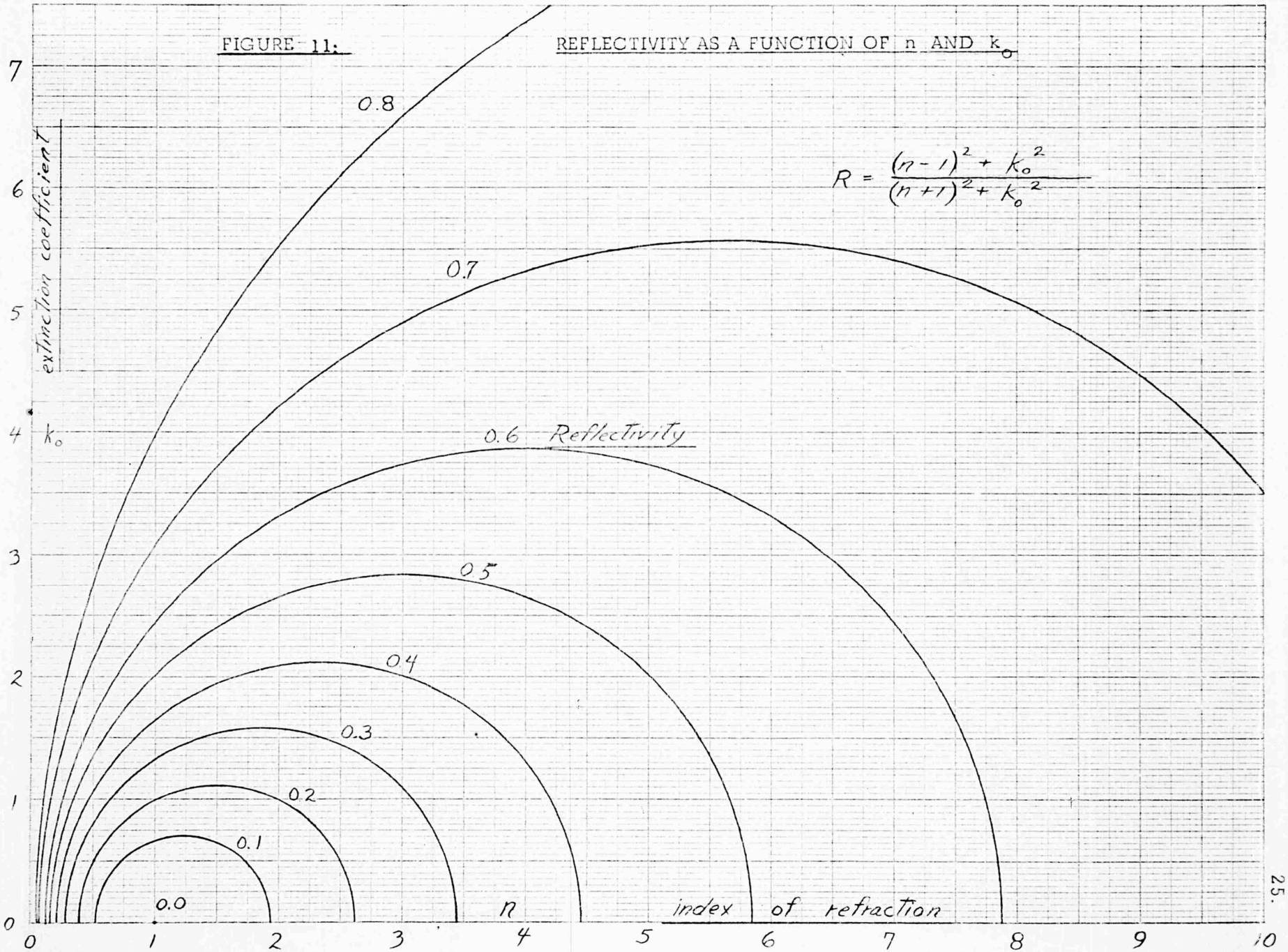

It is therefore possible to select semiconducting materials which will show reflectance at selected spectral regions from tables of band gaps.

Both dispersion data and band gap data have been used to select possible materials for selective reflectivity in the ultraviolet. In Fig. 12 are shown materials with high dispersion in the visible and therefore selective reflection in some part of the ultraviolet. In Fig. 13 the band gap is plotted versus the reciprocal of the wavelength and the wavelength of the absorption edge for a number of materials. The cut-off point desired for high reflection in the ultraviolet is 0.46 microns, and materials with absorption edges near this such as zinc selenide are most promising. Compounds shown more than once in Fig. 13 have more than one reported band gap value.

Materials that are transparent in the range from 0.46 to 1.1 microns are dielectric materials with indices of refraction between 1.5 and 4. It is apparent from Fig. 11 that for these materials an extinction coefficient between .3 and 4 is required for 60% reflectivity. The optical properties of two possible materials, CdS and ZnS, are known and the reflectivities have been calculated. These data are shown in Fig. 14 and Fig. 15. The reflectivity is low and does not show a sharp cut-off at the long wavelength edge.

Electronic absorption does not give rise to absorption of large enough magnitude to result in high selective reflectivity as required.

4.3 Emissivity

Most dielectric and semiconducting materials can be treated as "gray" bodies in that the distribution of radiation as a

FIGURE 12: DISPERSION CURVES OF VARIOUS MATERIALS

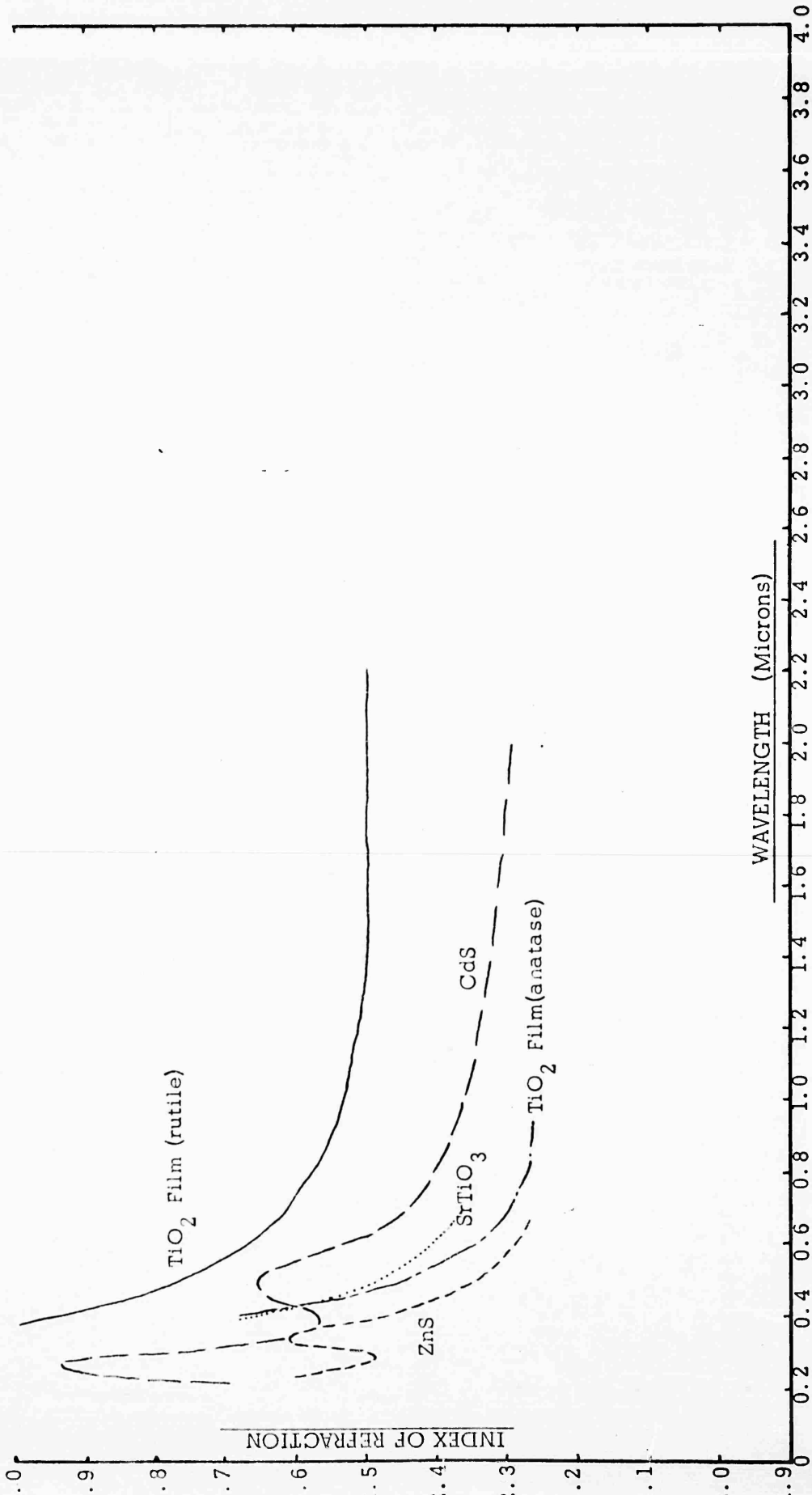

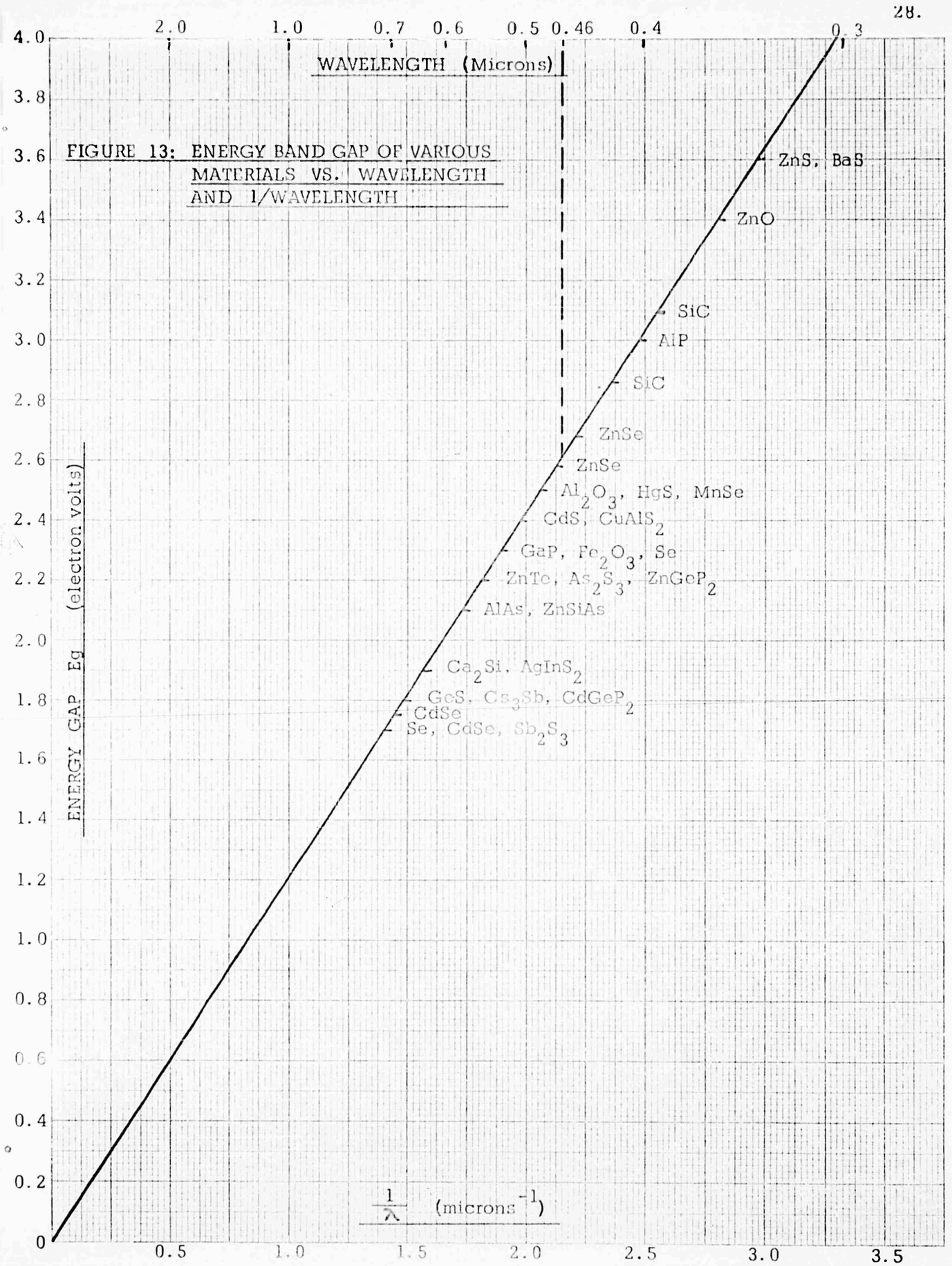

FIGURE 13: ENERGY BAND GAP OF VARIOUS MATERIALS VS. WAVELENGTH AND 1/WAVELENGTH

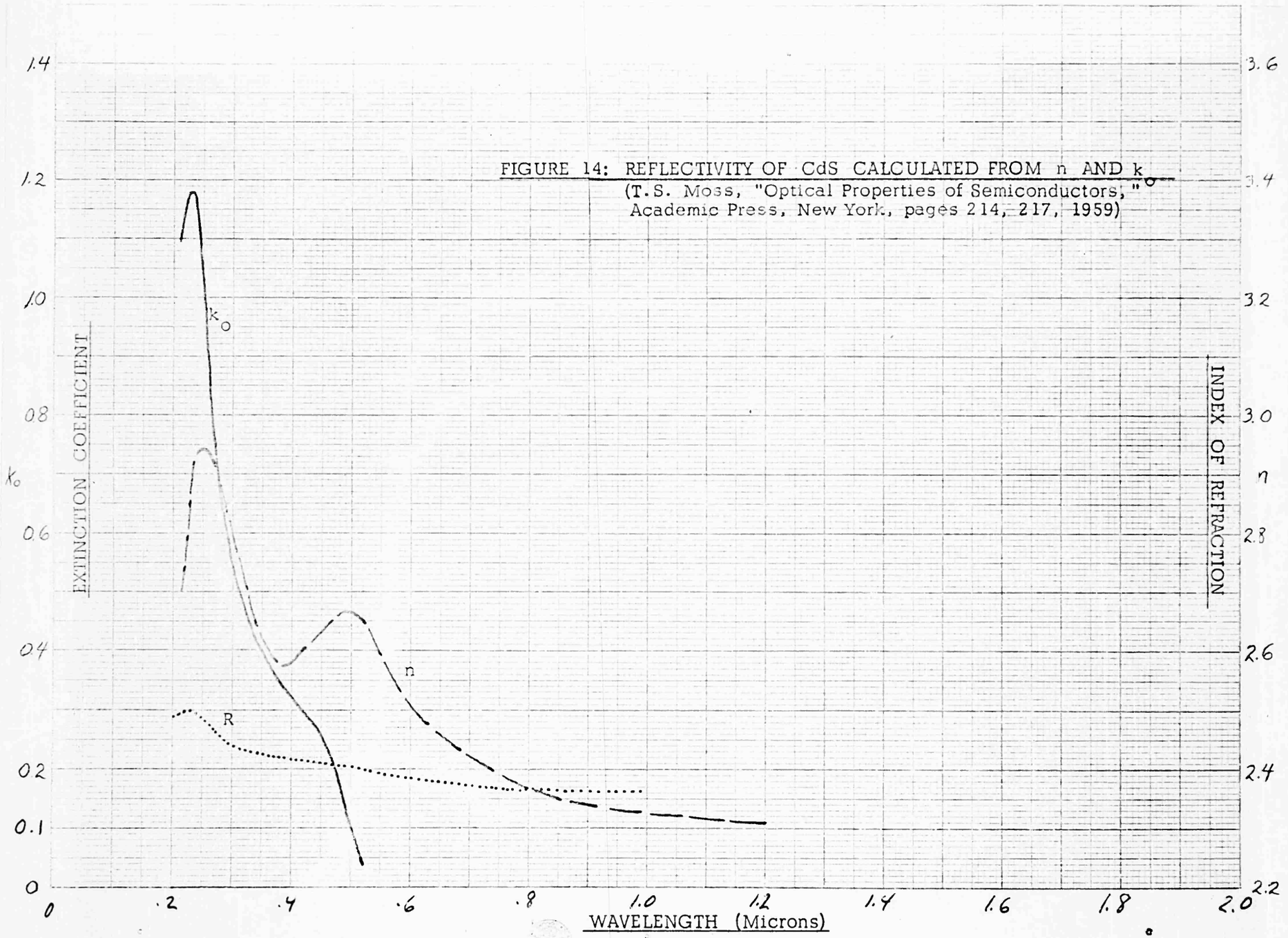

FIGURE 14: REFLECTIVITY OF CdS CALCULATED FROM n AND k_o
(T.S. Moss, "Optical Properties of Semiconductors," Academic Press, New York, pages 214, 217, 1959)

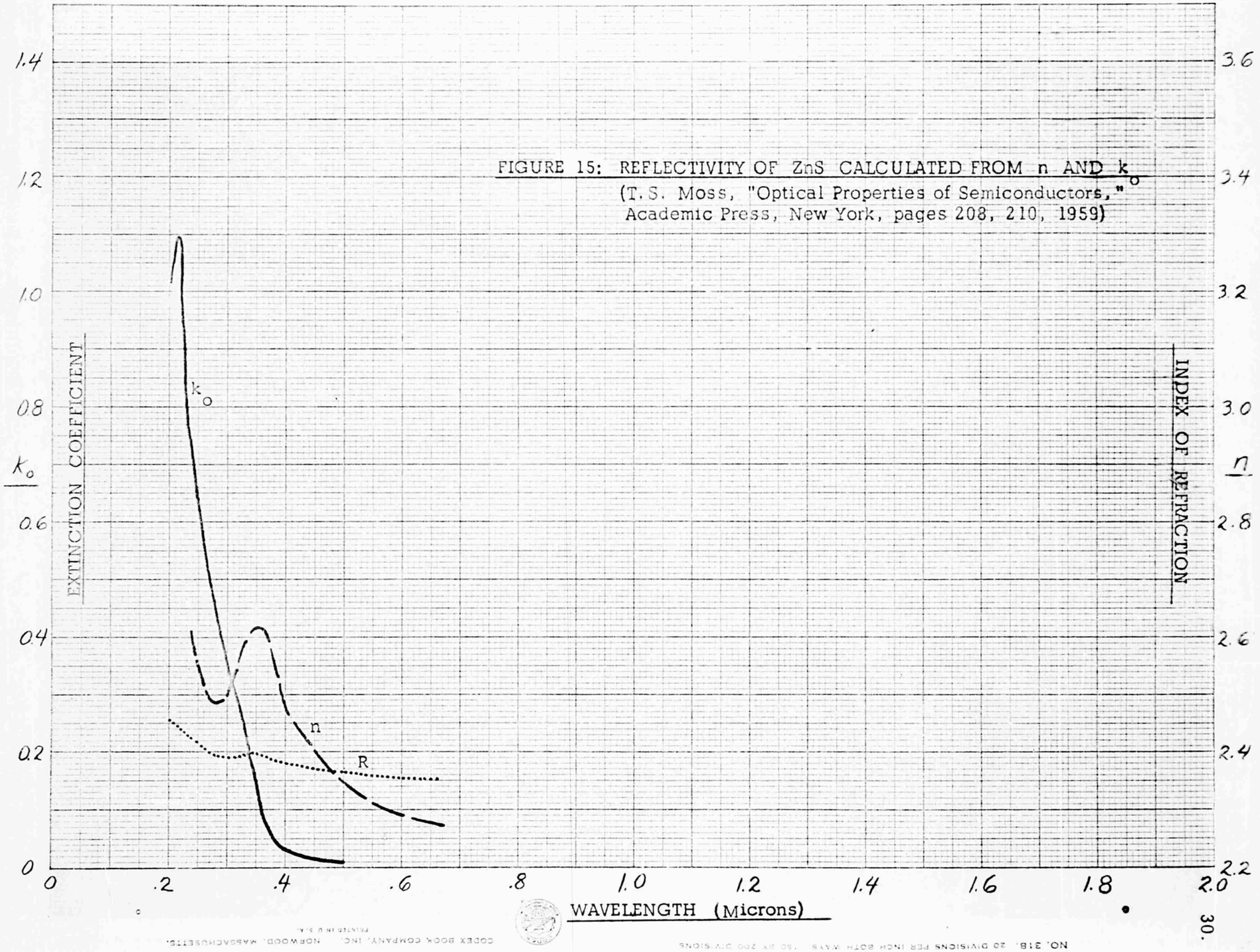

FIGURE 15: REFLECTIVITY OF ZnS CALCULATED FROM n AND k_o
(T. S. Moss, "Optical Properties of Semiconductors," Academic Press, New York, pages 208, 210, 1959)

function of wavelength is the same as for a black body but the intensity of radiation is reduced by a constant ratio for each wavelength. The emissivity (ϵ) of a body is the ratio of the radiation emitted by the body in any direction or in all directions to that emitted by a black body.

Emissivity (ϵ) is related to reflectivity (R) by Kirchoff's law,

$$R_{\phi} = 1 - \epsilon_{\phi} \quad , \qquad (1)$$

in which the angular dependence of R and ϵ are represented by the subscript ϕ, the angle of incidence. Combining this with Fresnel's formula,

$$R = 1/2 \frac{\sin^2(\phi - \chi)}{\sin^2(\phi + \chi)} \left[1 + \frac{\cos^2(\phi + \chi)}{\cos^2(\phi - \chi)} \right] \qquad (2)$$

where

ϕ = angle of incidence,

χ = angle of refraction

and the expression for the normal reflectivity of a non-absorbing medium

$$R = \left(\frac{n - 1}{n + 1} \right)^2 \quad , \qquad (3)$$

the emissivity may be calculated as a function of ϕ and n, assuming that n is independent of ϕ. This calculation is complicated, but has been made.[3] The results are shown graphically in

Fig. 16. The distribution of energy radiated follows Lambert's cosine law for a black body. The angular distribution of radiation for "gray" bodies with indices of refraction of 1.41 and 2 are compared with that of a black body at the same temperature in Fig. 17.

The radiation of energy as a function of the angle of incidence was obtained using the emissivities plotted in Fig. 16. The ratio of the area under the radiation distribution curve for a "gray" body to that of a black body gives the total emissivity of the "gray" body. The total emissivity (ϵ_T) and the normal emissivity ($\epsilon_{\phi=0}$) of materials with various indices of refraction are shown in Table II.

TABLE II

n	1.0	1.41	2.0	3.0	4.0	5.0
ϵ_T	1.00	0.92	0.83	0.72	0.63	0.56
$\epsilon_{\phi=0}$	1.00	0.97	0.89	0.75	0.64	0.56

These results can be used as a guide in selecting materials for producing high emissivity, although they are not sound theoretically for several reasons. Equation (1) assumes zero transmission while Equation (3) assumes complete transmission and also is limited to normal incidence only. Further, in the derivation it was assumed that n is independent of ϕ. This is not true, since $R = f(\phi)$ in Equation (1), and $R = f(n)$ in Equation (3); therefore $n = f(\phi)$.

If the transmission of a coating is zero, the emissivity of a composite structure is determined by the coating alone. If the transmission of a coating is large the emissivity will be determined by both the coating and the substrate.

FIGURE 16: EMISSIVITY AS A FUNCTION OF ANGLE OF INCIDENCE (Φ) FOR NON-ABSORBING MATERIALS WITH VARIOUS INDICES OF REFRACTION (n)

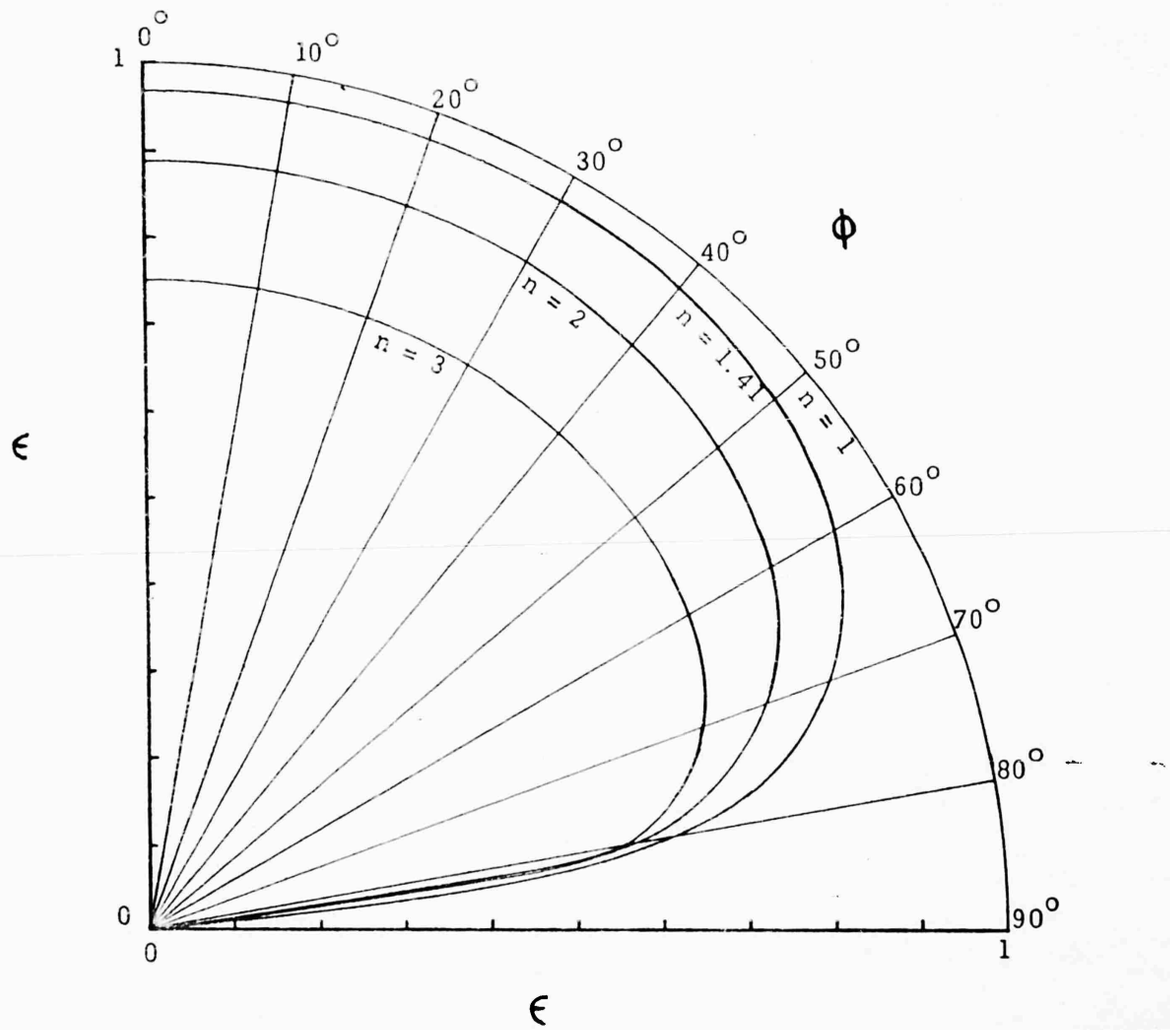

FIGURE 17: DISTRIBUTION OF RADIATED ENERGY AS A FUNCTION OF ANGLE OF INCIDENCE (ϕ) FOR MATERIAL WITH VARIOUS INDICES OF REFRACTION (n)

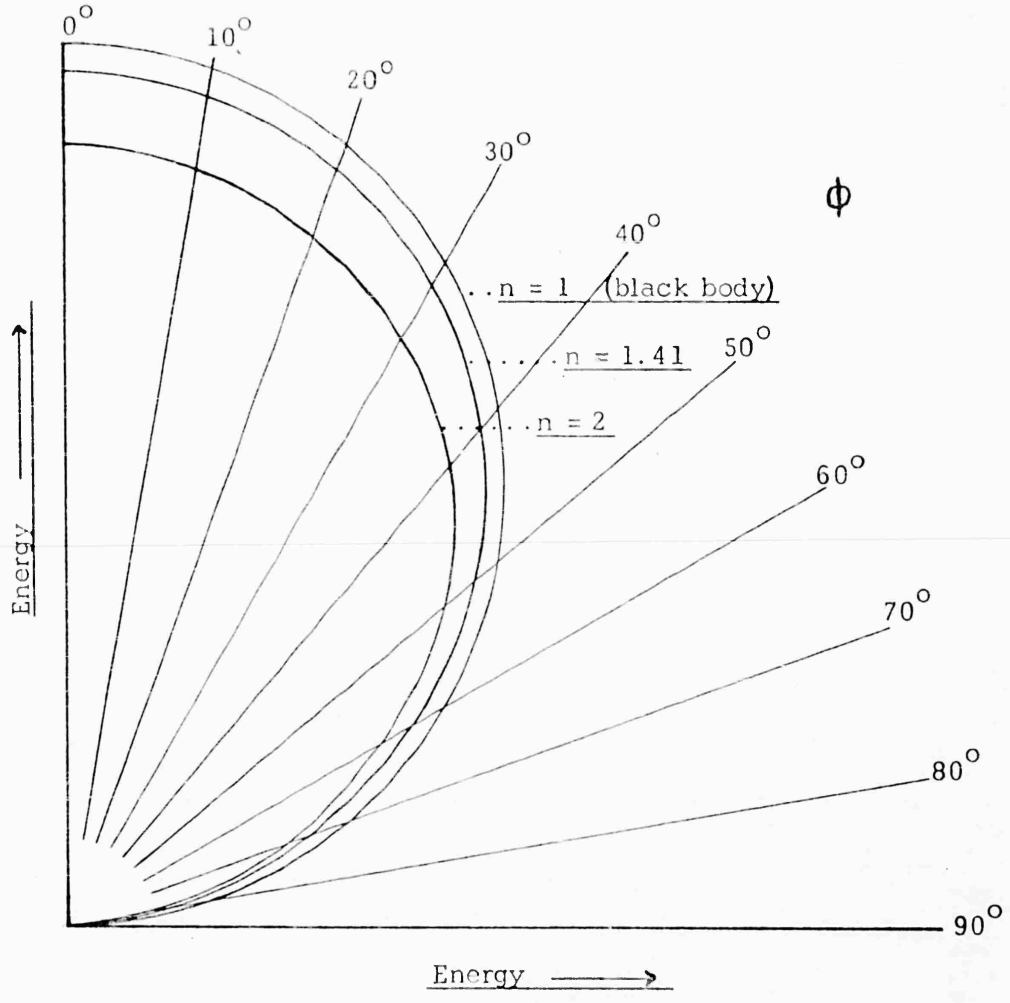

Two kinds of coatings for increasing the emissivity of solar cell surfaces are suggested by these conclusions.

1) Thin Film Coatings. Thin non-opaque films with indices of refraction intermediate between the substrate and air may be applied to the surface to increase emittance and decrease reflectance. This will result in a combination having an emissivity intermediate between that of the cell and of the coating material. However, if a coating could be prepared with an index of refraction changing gradually from that of the substrate to unity, an emittance of one would be obtained.

2) Thick Coatings. Coatings thick enough to be opaque or approximately so in the desired infrared range can be applied to the cells to produce high emittance. The emittance of these coatings will be determined by the properties of the coatings alone. The glass cover slides presently in use are an example of this approach. The optimum coating of this type is one with a minimum index of refraction in the infrared and without important reflection peaks in the infrared.

4.4 Summary of the Theoretical Conclusions

The conclusions of the various theoretical considerations can be briefly summarized for each of the spectral regions of interest. The primary requirement that any coating must have a high transmittance from 0.46 to about 1.1 microns limits possible materials to dielectrics and to semiconducting materials having no absorption band in the desired transmission range.

The absorption and reflection of radiation in the ultraviolet arises from oscillations of bound electrons in the electromagnetic field of incident light. These electrons are bound in varying degrees to the atoms or ions of the material and give rise to a low, broad reflectivity

peak. The maximum reflectivity expected is less than 0.5 and the cut-off is not sharp.

In the infrared, from about 1 to about 20 microns, reflectivity is associated with atomic vibrations within a molecule, crystal or polymeric structure. The highest resonant frequencies found are those for light atoms bound to hydrogen atoms, as in water or in hydroxyl groups, or for bonds between light atoms which have exceptionally high force constants, as in CO or CO_2. However even for such bonds the highest resonant vibration frequencies correspond to wavelengths of 2 to 4 microns. From the foregoing considerations, no solid dielectric material may be expected to have high reflectance at the wavelength required, namely 1 to 2 microns.

In the infrared beyond 4 microns a maximum emissivity is required. The requirements for a single material coating are that the coating be opaque in the thickness used and in the spectral region of interest, and that it have the lowest possible index of refraction. A low index of refraction in the infrared may be generally inferred from a low dielectric constant. On this basis many organic compounds, silicones and certain inorganic compounds will have low refractive indices in the infrared. The selection of materials among these must be made principally on the basis of transmission requirements from 0.46 to 1.1 microns, of stability in a space environment, and of stability in air.

5 Experimental

5.1 Thin Film Coatings

As a result of previous considerations the possible use of thin coatings was considered, with the objective of increasing emissivity.

Thin films of several compounds including MgF_2 were vacuum deposited onto cell surfaces. These were deposited initially with the expectation that any of these thin films would increase the emissivity and decrease the reflectivity of the cell surface. In addition higher index of refraction films of TiO_2 were deposited by the hydrolysis of $TiCl_4$, both separately and in combination with vacuum deposited coatings of MgF_2. TiO_2 has broad absorption and a reflectivity band in the near ultraviolet which overlaps into the visible.

Initial reflectance measurements showed a general increase in reflectance for the coated solar cell surfaces through the visible and near infrared. This result was unexpected, assuming the index of refraction of a cell surface to be at all close to the value of 3.44 commonly given for silicon. At the same time, assuming an index of refraction of 3 results in a calculated reflection of 25%, while the observed reflectance of solar cell surfaces in the visible is less than 10%. Because of these questions the optical properties of the front surface of solar cells were investigated in more detail.

5.2 Solar Cell Surfaces

The exposed surface of a presently produced silicon solar cell consists of highly doped, low resistivity, p-type material. This material is very strongly absorbing and therefore most readily studied using light reflection techniques.

The previous results using thin films would be expected if the index of refraction of the cell surface was less than one, analogous to a metal. In this case any transparent, dielectric coating on a cell would have an index greater than one, and would increase the surface reflectance. A simple apparatus was constructed to estimate the index of refraction of the solar cell surface at a wavelength of 0.59μ.

The method used, described by Jenkins and White,[4] requires measurements of the polarizing angle for a reflected light beam. In this method, the principal angle of incidence $(\bar{\phi})$ and the principal azimuth $(\bar{\psi})$ are measured, and the index of refraction (n) and the extinction coefficient (k_o) are computed from the relations

$$n\sqrt{1+\frac{k_o^{\,2}}{n}} = \sin\bar{\phi}\tan\bar{\phi}$$

$$k_o = n\tan 2\bar{\psi}.$$

With the simple equipment used the measurements of $\bar{\phi}$ and $\bar{\psi}$ required visual estimates of the maximum extinction of the reflected light beam, resulting in inaccurate determinations of $\bar{\phi}$ and $\bar{\psi}$ and therefore of n and k_o. However, typical values found for the index of refraction were less than one, and were in the neighborhood of 0.7 to 0.9.

Subsequently Hall[5] published evidence to show that the index of refraction of the surface of silicon solar cells is also less than one for wavelengths greater than 1μ. Thin anti-reflecting films can not therefore be used to increase emissivity in the infrared beyond 1 micron. At wavelengths less than 1 micron, Hall's method for determining the index is not applicable.

These index determinations are important because they show that the reflectance of solar cells in the visible and infrared can not be decreased by applying a single non-absorbing coating to the surface. This conclusion results from a consideration of the equation for reflectivity

$$R = \frac{(n_1 - n_2)^2 + ko^2}{(n_1 + n_2)^2 + ko^2} = 1 - \epsilon \quad .$$

When there is no coating on the cell, n_2 is unity (in air or vacuum) and a reflectivity for the cell can be calculated using the index of refraction, n_1, and the extinction coefficient, k_o, for the cell surface. When the first layers of any non-absorbing coating are applied to the cell surface the value of n_2 becomes greater than unity and the reflectivity increases, thereby decreasing the emissivity. Therefore, it is not possible to increase emissivity by modifying the properties of the cell surface using a thin coating. Rather the coating itself must provide a high emissivity to the coated cell.

5.3 Thick Film Coatings - General Considerations

Thick films as used here are films of thickness sufficient to provide the desired optical properties because of their own material properties and not only the modification of interfaces. Such a coating must be thick enough to be opaque (small transmission) to radiation of wavelengths from 4 and 40 microns in order to provide the maximum emissivity of the material.

The transmission is expressed by

$$T = e^{-\alpha x}$$

where α is the absorption coefficient and x is the thickness. T in this equation is independent of reflections at various interfaces. For

low transmission it is necessary that the product αx be large. However because the reflection of the surface depends on both α and the index of refraction of the material, a large α will give rise to large undesirable reflection losses at the surface. The product αx must therefore be made large by increasing the thickness x to the order of 1 to 10 mils.

The microscope cover glasses currently being used on solar cells are thick films. However, as shown subsequently the emissivity of the glass is decreased by the anti-reflection coating applied to the front surface.

The possibility of using thick coatings of low index of refraction crystalline materials was then considered. While compounds such as LiF, MgF_2, CaF_2 and others have low indices of refraction and should therefore show low reflection losses and high emissivity, all show anomalous dispersion curves in the infrared. This would serve to reduce the maximum emissivity. In addition, serious difficulties arise in applying adherent coatings of the necessary thickness, as well as questions of over-all environmental stability. For these reasons further work with this type of coating was discontinued while other approaches were considered. The possible use of metal oxides was also rejected for these same reasons plus the increased difficulty in producing transparent coatings of the necessary thickness.

5.4 Polymer Coatings

Organic polymers, including silicones, have high emissivities as a group due to their generally low index of refraction and to the fact that they do not yield intense reflectivity peaks in the infrared. These materials would be highly desirable from the point of view of their emissivity and ease of application. However a major question

with such coatings concerns their stability to a space environment, including direct solar radiation, the high vacuum in space, electron and proton bombardment, and resistance to thermal shock.

Several studies have been made of various paint compositions for use on spacecraft which give a good idea of the relative stabilities of various polymers. (cf. 6) The results of these studies showed silicones, in comparison with other organic polymers, to have excellent stability when exposed to ultraviolet radiation in a vacuum. Silicones also have outstanding oxidation resistance and thermal stability, as well as stability to high energy radiation.

The stability to high energy radiation can be used as one guide in the selection of possible materials to be investigated, since any coating may be exposed to both electrons and protons in the Van Allen belts, as well as to extremely high energy protons resulting from solar flares. Many studies of the stability of polymers have been carried out using reactor radiation, Co^{60} γ sources and electron beams in accelerators.[7] These studies have shown that aromatic hydrocarbons are an order of magnitude more stable to radiation than are aliphatic hydrocarbons. This radiation insensitivity has been ascribed to the resonant structure of the benzene ring which enables considerable excitation energy to be absorbed without bond rupture. It may even be considered that loss of an electron still leaves a sufficient number of bonding electrons to leave a stable structure. This protection can even be extended to neighboring non-aromatic hydrocarbons if their lowest excited energy state is above that of benzene. Polymers with high aromatic contents are therefore the most stable to radiation. Polystyrene is the most radiation resistant of the organic polymers, absorbing about 2000 ev per cross link formed at room temperature for either pile, γ , or X-ray irradiation. Most other organic polymers require one to two orders of magnitude less energy per cross link or chain rupture. High phenyl content sili-

cones are comparable with polystyrene in radiation resistance, due to the phenyl content, and possess the added advantage of outstanding thermal stability. (Polystyrene begins to distort readily under load at $80^{\circ}C$.)

The aromatic content of a silicone polymer also contributes to stability towards ultraviolet radiation. Degradation from ultraviolet radiation is minimized if the material has a low absorption, and if a mechanism other than bond rupture is available for dissipation of absorbed photons. It can be seen from Fig. 18 that Resin XR6-2044 has a very slight absorption to 0.3μ, although all polymers become good absorbers below 0.25μ. Although much of the radiation is absorbed by excitation of the phenyl groups and degradation to heat, the remaining energy effects cross linking in the polymer.

The cross linking reaction involves primarily the breaking of Si-C and C-H bonds. Subsequently the free radicals formed react to form Si-C-Si, Si-C-C-Si, or Si-Si cross links, with the evolution of H_2 or CH_4.

However, these reactions do not explain the increased absorption found in coatings which have been irradiated. In the course of this work it was found that prolonged exposure of silicone coatings to ultraviolet radiation usually results in the development of a broad absorption band centered in the ultraviolet at about 0.34μ. The responsible reaction or mechanism, or the possible dependence on impurities, have not been established.

5.5 Evaluation of Silicone Coatings

From the foregoing discussion it was concluded that of the possible polymeric coatings, silicones as a group offered the most promise of meeting all environmental requirements. From preliminary measurements of both transmission and reflectance, it appeared

FIGURE 18: TRANSMISSION OF SILICONE

XR6-2044 Resin, 0.046 inches thick, with no substrate.
Curve not corrected for reflection losses.

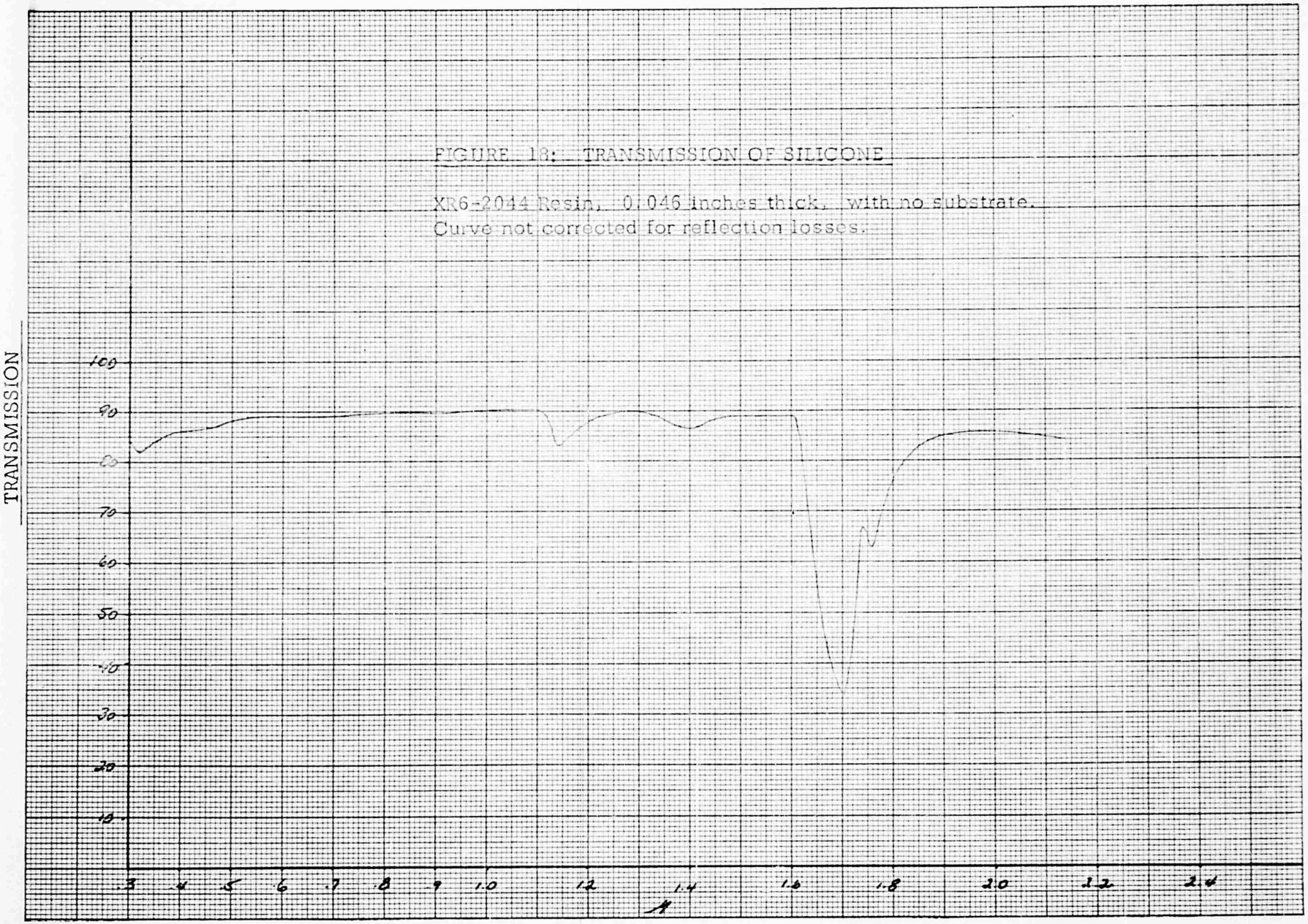

that a silicone coating alone should give solar cell performance equivalent to a coated cover glass, but at a much smaller cost. The major question concerned stability in a space environment. A series of evaluation tests was therefore initiated to select the commercially available silicone most suitable for coating cells so this could be more exhaustively evaluated.

Resins investigated included Dow-Corning A-4000, 805, 40C, 980, Q30040, XR 6-2044, 23 and 2-69, and Union Carbide XR-630, R-620, and C-25. A preliminary evaluation of the resins was made by applying these to glass slides; rejecting those that showed visual absorption, or that could not be cured to produce firm, tack-free coatings. Additional simple environmental tests included the effects of exposure to water and steam, and thermal shock resistance when coated slides enclosed in an evacuated tube were quenched from room temperature into liquid nitrogen. Of the materials tested the resins XR 6-2044, 805 and A4000 withstood all of the tests performed. Measurements of the transmission and reflectance of these coatings showed all to be very similar.

On exposure of these coatings to radiation from a Hanovia, 800-watt, high pressure Xenon arc overnight, it was found that severe crazing of the coatings occurred, with some visual discoloration. It was found that identical crazing occurred in the absence of U.V. radiation to samples which were heated to moderate temperatures in an air stream containing ozone from an electrodeless discharge. Similar crazing also occurs on heating these coatings at $250^{\circ}C$. in air for times of the order of 1000 hours. These results can be attributed to rapid cross linking when the silicone resin is exposed to ozone at elevated temperatures, and to somewhat less rapid cross linking when heated in the presence of oxygen. These results emphasize the great importance of rigorous atmosphere control during ultraviolet irradiation tests.

Information received from Dow-Corning stated that XR 6-2044 had a high aromatic content, and the optimum combination of radiation resistance and thermal shock resistance. In addition this resin was of particularly high purity, which would minimize radiation degradation through impurities. This resin was therefore selected for the initial extended ultraviolet radiation tests in controlled atmosphere, until satisfactory test procedures were established.

The recommended curing cycle for several of these coatings, including XR 6-2044, required heating to 250°C. for several hours. While heating to this temperature does not affect the solar cell junction, the electrodes and contacts to the silicone can be affected, particularly since the soft solder used for electrode connections melts at 189°C. The initial studies of coatings which were cured at 250°C. did show a degradation in cell output which was traced to increased electrode contact resistance rather than to any direct effect of the coating. Steps were therefore taken to lower the required curing temperature to about 150°C., since the curing cycle for an assembled panel would have to be below the melting temperature of the solder.

Tests were run on a group of nominal 12% cells comparable to those being used on Ranger panels. It was found that heating these for several hours to the melting temperature of the solder, 189°C., gave no decrease in power output. A curing cycle below this temperature should therefore have no effect on cell efficiency.

In order to cure at 150°C. it was necessary to use a catalyst. Several catalysts supplied by Dow-Corning for other resins were tried with resin XR 6-2044, including one specifically recommended. This latter catalyst, designated XY15,* was found to give the best

*This catalyst is an organic amine of unspecified composition.

cure in three hours at 150°C., used in 0.3 weight percent concentration. All sample coatings of this resin prepared after the initial exploratory tests used this catalyst and final cure. Coatings thicknesses of 10 mils and more were successfully applied by curing for one hour at 150°C. between successive coats averaging one to two mils in thickness. These coatings were prepared using both brush and spray techniques.

5.6 Ultraviolet Radiation Tests

Although some preliminary ultraviolet radiation stability tests were performed using a hydrogen arc source, all tests discussed in this report were done using a Hanovia, No. 418 C, 800-watt high pressure Xenon arc. This arc was selected because of its continuous spectrum in the ultraviolet, which is a fair approximation to sunlight, and because of the high intensity of radiation in the ultraviolet. Energy comparisons can be made using published data for the Xenon arc* [8], for sunlight at the surface of the earth [8], and for sunlight in space.[1] These are summarized in Table III.

TABLE III: ULTRAVIOLET CHARACTERISTICS OF XENON ARC

	Test Distance (inches)	Total energy-milliwatts/cm^2	
		$<0.4\mu$	$<0.35\mu$
Sunlight, Earth's surface:	----	4.24	1.18
Sunlight in space:	----	13.6	6.46
Xenon Arc, no filter:	10	4.05	1.49
Xenon Arc, no filter;	5.4	13.9	5.12
Xenon Arc, no filter:	1.75	132	48.7

* The manufacturer has stated that the arc used in this work, No. 418C, has the same light output as No. 507C1 considered in Ref. 2.

Arc energies at different distances have been calculated using an inverse square relationship, even though the arc has a cross section area of about 1 mm. by 8 mm. As a check on the accuracy of this assumption, a relationship was derived by L. DeVore to a second order approximation, assuming a line source of finite length, and assuming the cosine law for the variation of intensity with angle. This expression is

$$W = \frac{2\pi I ab^2}{S\sqrt{S^2+a^2}} ,$$

in which W is the energy incident on a surface of radius b at a distance S from the arc, and 2a is the length of the arc. For sample distances of about 1.75 inches, or something more than 5 times the arc length, this reduces to the inverse square law.

The first extended ultraviolet radiation tests using the Xenon arc ran a total of 117 hours. Resin XR 6-2044, using XY15 catalyst and cured at 150°C. for 3 hours, showed no visible degradation at the end of this time. The entire exposure was done using a Corning ultraviolet transmitting filter, No. 5850, to absorb infrared radiation from the arc. The samples were located 3 inches from the arc, and were contained in quartz tubes in a flowing stream of argon to provide both cooling and an inert atmosphere. Previous survey runs showed that the equilibrium coating temperature was about 50°C. with this test arrangement.

The complete exposure was not done continuously but was interrupted on numerous occasions because of several failures of the power supply and starter, as well as to permit examination of the samples. The total exposure was estimated to be equivalent to about 7 sun days in space. However, the estimation of equivalent sun days in space is difficult for several reasons. Any filters that

are used lose in transmission due to solarization, and it was found that the Corning filter used in this test decreased in transmission by about 50% after 60 hours exposure to the Xenon arc. The quartz sample enclosure also decreases in transmission. Examples of these changes are shown subsequently in Figs. 21, 22, and 24. In addition the arc manufacturer states that the radiant energy output of the Xenon arc decreases by 50% in 200 hours under A.C. operation. However, nothing is known of the change in spectral distribution of the arc during this time. After 20 to 30 hours of operation, a slight violet tint can be seen in the quartz envelope of the arc, showing that absorption bands are being produced in the ultraviolet. All of these factors result in considerable uncertainty in interpretation of these results. However, the possibility of analyzing and monitoring the arc radiation was beyond the scope of this work.

Subsequent tests attempted with this experimental arrangement were inconclusive because of inadequate atmosphere control. New sample cells were then designed in which two quartz windows one-inch in diameter by one-eighth inch thick were mounted in a metal cylinder so that the space between windows could be kept under a positive pressure of argon. This complete cell could be mounted on the spectrophotometer to permit transmission measurements without disassembly, and without affecting the argon atmosphere. The test coating was applied to the inner side of one window, the reverse side of this window being water-cooled during irradiation.

Two of these cells were assembled, with a 3-mil coating of XR 6-2044 resin in one, and a 6-mil coating in the second. An irradiation run was made which continued for a total of 246 hours. Details of this run are given in Table IV.

TABLE IV: ULTRAVIOLET IRRADIATION TEST, XR 6-2044 SILICONE COATING

# of Run	Duration of Run-Hours	Distance from Arc-Inches	Arc Age at Start-Hours	3-mil Coating		6-mil Coating	
				Filter	Filter Age at Start-Hours	Filter	Filter Age at Start-Hours
1	18	1.75	250	(1)	~60	---	---
2	17	1.75	268	(1)	~78	(1)	~60
3	63	2.5	40	(1)	0	(1)	0
4	46	2.5	103	(1)	0	(1)	0
5	17	2.5	149	(1)	0	(1)	0
6	21	2.5	166	(2)	0	None	---
7	64	2.5	187	(2)	64	None	---

(1) Corning ultraviolet transmitting filter no. 5850. See Fig. 24.

(2) Heat absorbing glass, Edmund Scientific Co. no. 4073. See Fig. 25.

The effects of this irradiation run are shown in Figs. 19 through 23. The argon atmosphere was maintained without interruption throughout the entire duration of the test and throughout all transmission measurements on the assembled cells. Figs. 19 and 20 show the decrease in transmission of the assembled cells during the course of the irradiation. Figs. 21 and 22 show that a very significant part of the loss in transmission results from increasing absorption of the fused quartz windows and substrates.* Combining these curves with those for the transmission of the coatings on the fused quartz substrates, immediately after disassembly of the cells, yields curves for the final transmission of the silicone coatings alone, corrected for transmission losses, as shown in Fig. 23. This figure shows that no change occurred in the transmission of the 3-mil coating throughout the entire 251 hours of irradiation. The departure of this curve from 100% is within the accuracy of the measurements; values below 0.6μ were obtained with the photomultiplier detector, those above 0.6μ with the thermocouple detector.

Although the transmission of the 6-mil coating has decreased considerably, the transmission of the assembled cell in Fig. 20 shows that no change in the coating occurred in the first 143 hours of irradiation. These changes began only after removal of the filter. (See Table IV.) Removal of the filter changed three factors, all of which could contribute to accelerated degradation of the coating. These include: (1) Additional ultraviolet radiation of shorter wavelengths is incident on the cell. (2) The flux density in the ultraviolet is increased significantly. (3) A large flux of infrared radiation is now incident on the cell, resulting in an increase in the coating temperature. This increase in temperature can be large, since about 75% of the total radiated energy of a Xenon arc is in the infrared.

---

* Subsequent annealing of the quartz substrate from the 6-mil coating at 200°C and at 600°C resulted in a further decrease in transmission of as much as 10%.

FIGURE 19: TRANSMISSION OF ASSEMBLED CELL WITH 3- MIL SILICONE COATING

Transmission curves shown are after 35, 166, 184 and 251 hours of irradiation.

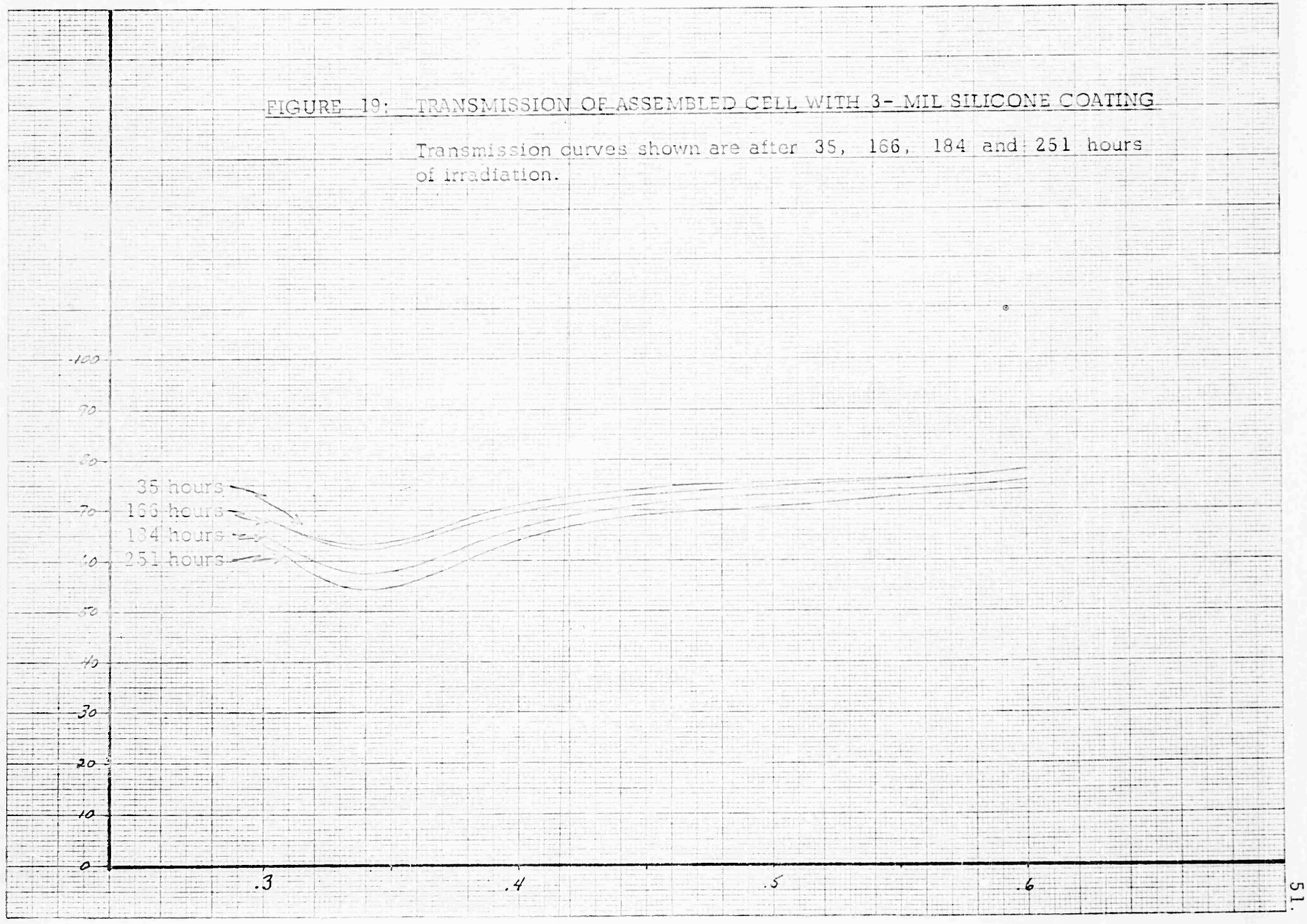

FIGURE 20: TRANSMISSION OF ASSEMBLED CELL WITH 6-MIL SILICONE COATING

Transmission curves shown after 17, 143, 164 and 228 hours irradiation.

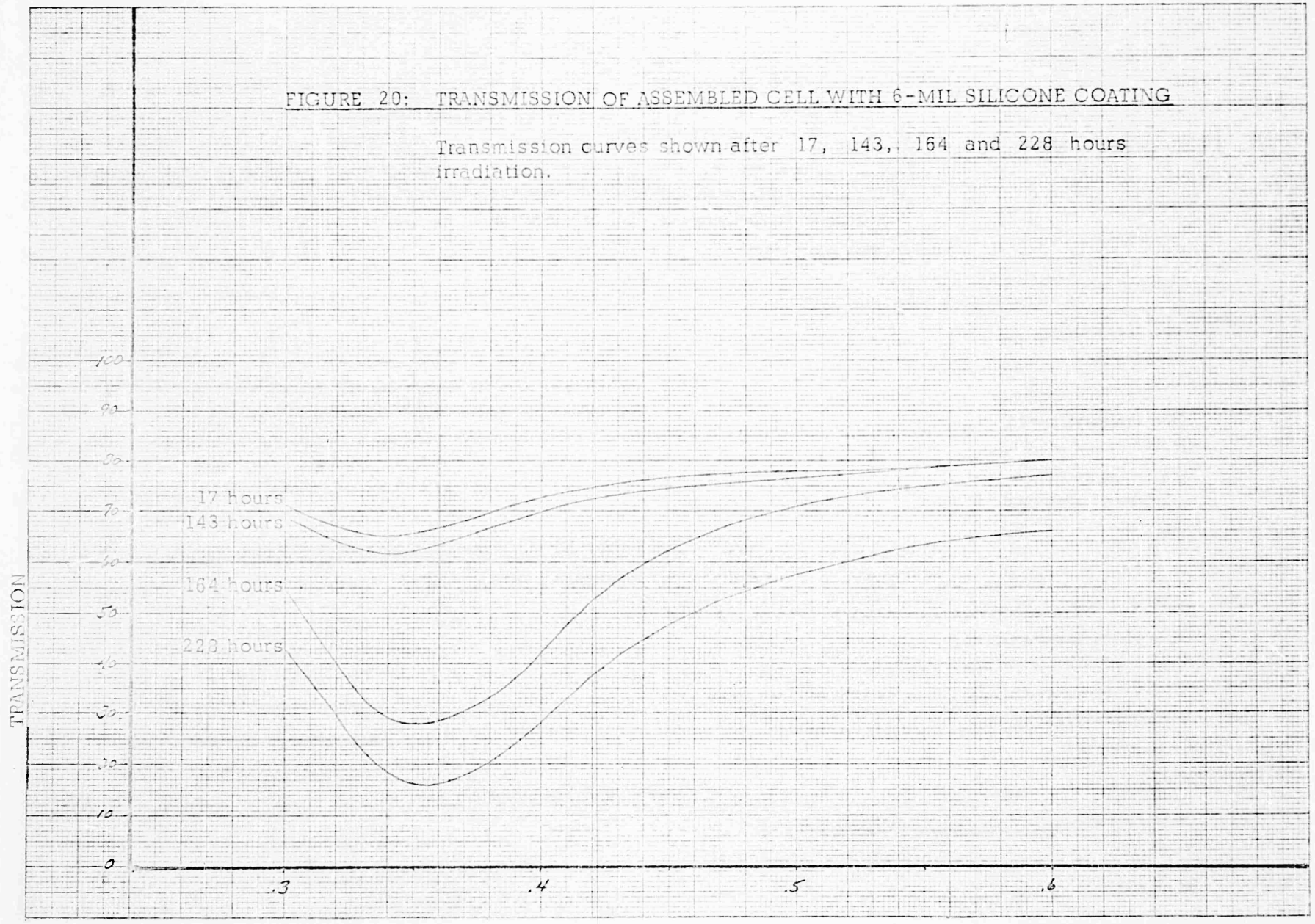

FIGURE 21: TRANSMISSION OF FUSED QUARTZ WINDOWS

Upper Curve- Quartz windows before irradiation.
Center Curve-Quartz window after 251 hours irradiation.
Lower Curve- Quartz substrate (from 3-mil coating) after 251 hours irradiation.

All windows are General Electric Type 101 Fused Quartz, 0.125-inch thickness.

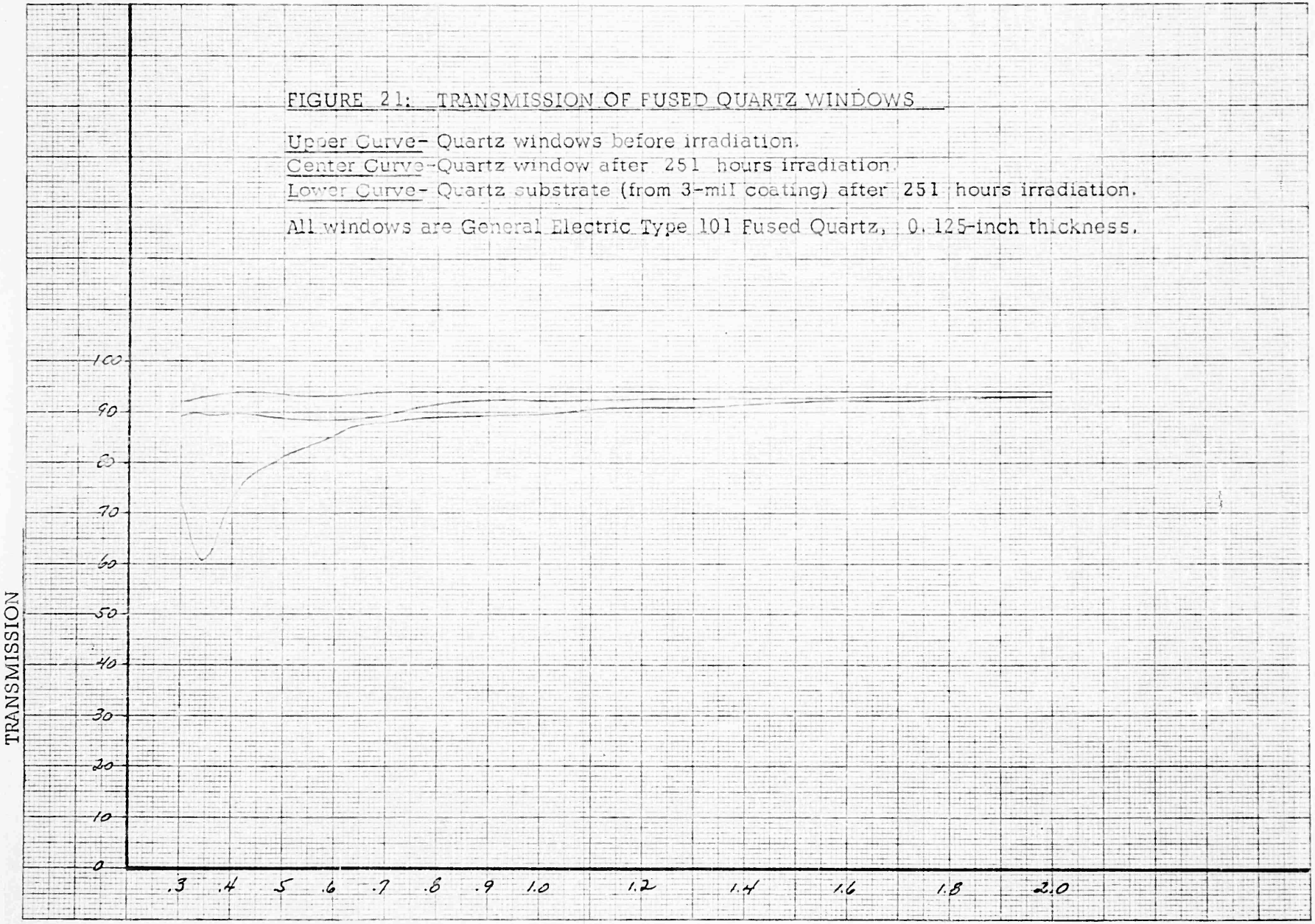

FIGURE 22: TRANSMISSION OF FUSED QUARTZ WINDOWS

Upper Curve- Quartz window before irradiation.
Center Curve- Quartz window after 228 hours irradiation.
Lower Curve- Quartz substrate (from 6-mil coating) after 228 hours irradiation.

All windows are General Electric Type 101 Fused Quartz, 0.125-inch thickness.

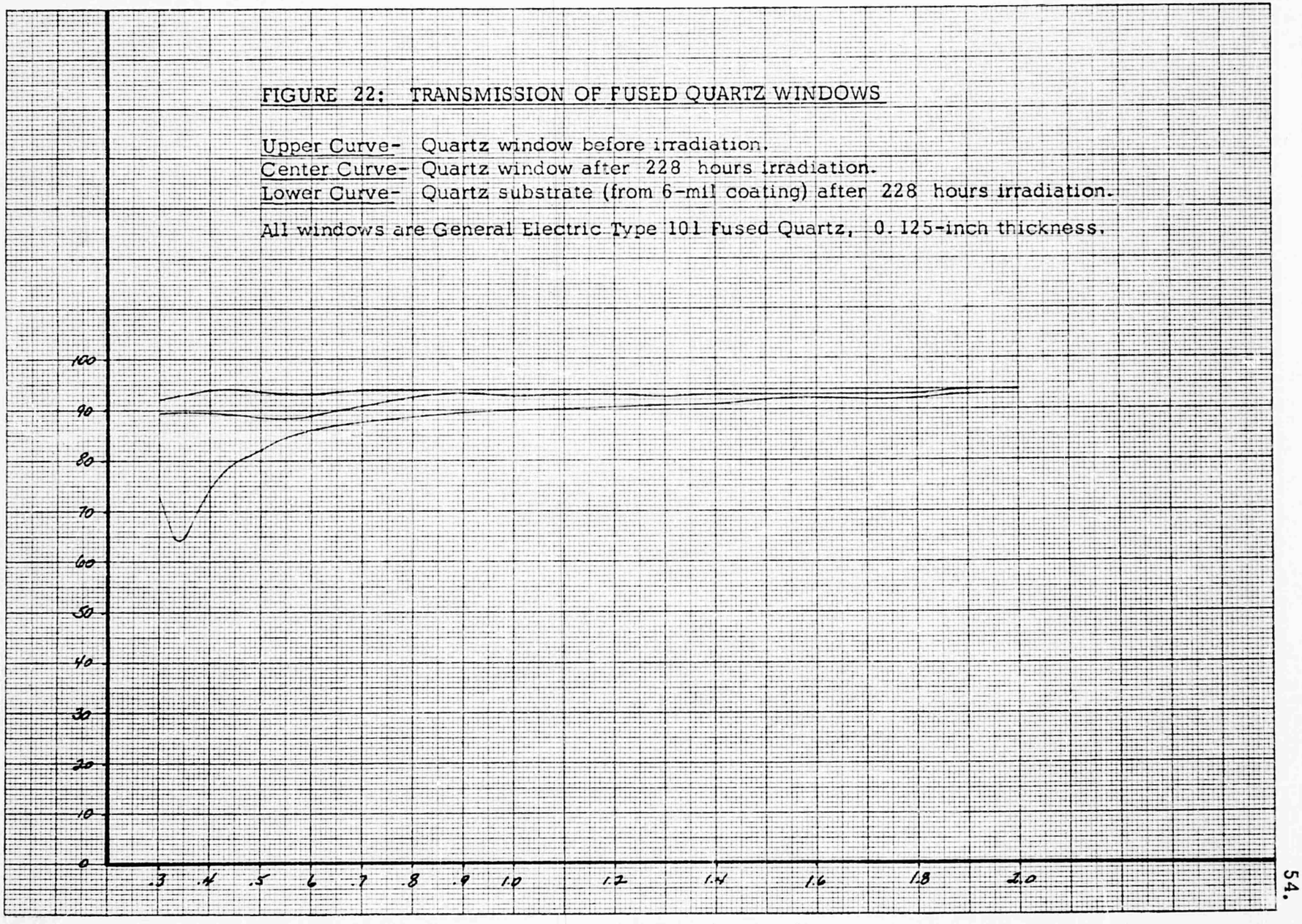

FIGURE 23: TRANSMISSION OF SILICONE COATINGS AFTER EXTENDED IRRADIATION

Curves are transmission of silicone coatings after about 21 equivalent sun days irradiation in space, corrected for transmission losses and absorption of substrate.

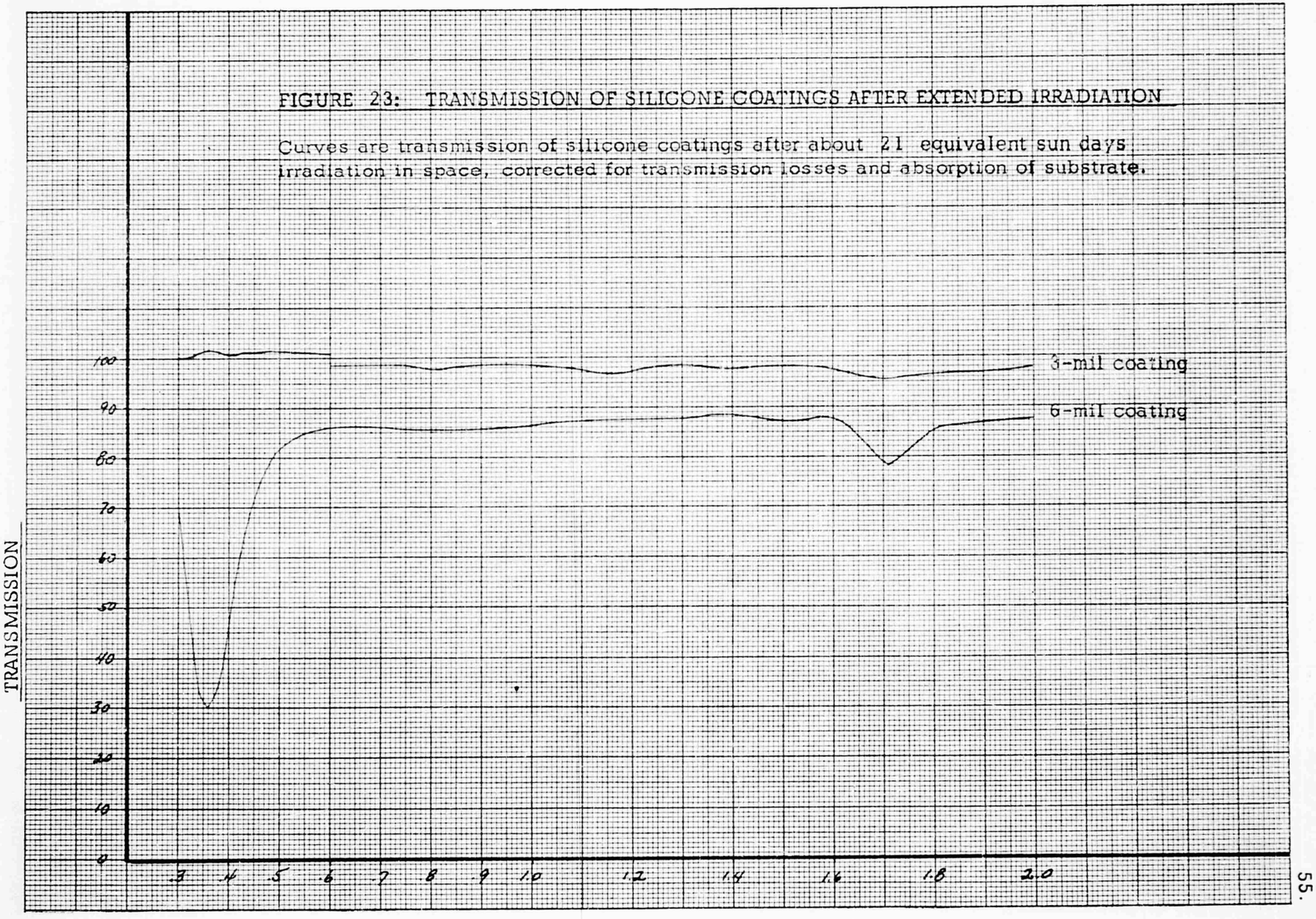

From the experiments performed to date, it is not possible to determine which of these factors effected the coating degradation. Additional controlled experiments will be required.

In estimating the total radiant flux below 0.45μ which was incident on the cells during this experiment, it is necessary to know the transmissions of the filters used. Typical curves are shown both before and after irradiation in Figs. 24 and 25. Combining this general information with the arc characteristics and test geometry, assuming the radiant flux below 0.45μ from the arc to decrease by 50% in 200 hours, it is possible to estimate the total radiant energy incident on the coatings. A figure for the equivalent sun days in space, considering radiant energy below 0.45μ only, can be calculated by combining this with data from Johnson's curve for the spectral distribution of sunlight in space.[1] This calculation results in 20 equivalent sun days for the 3-mil coating. For the 6-mil coating, the calculated exposure is 12 equivalent sun days with filters, and an additional 9 sun days without filters.

FIGURE 24: TRANSMISSION OF CORNING FILTER NO. 5850 BEFORE AND AFTER IRRADIATION

Curves shown are for two filters.
Upper curves are before irradiation.
Lower curves are after irradiation.

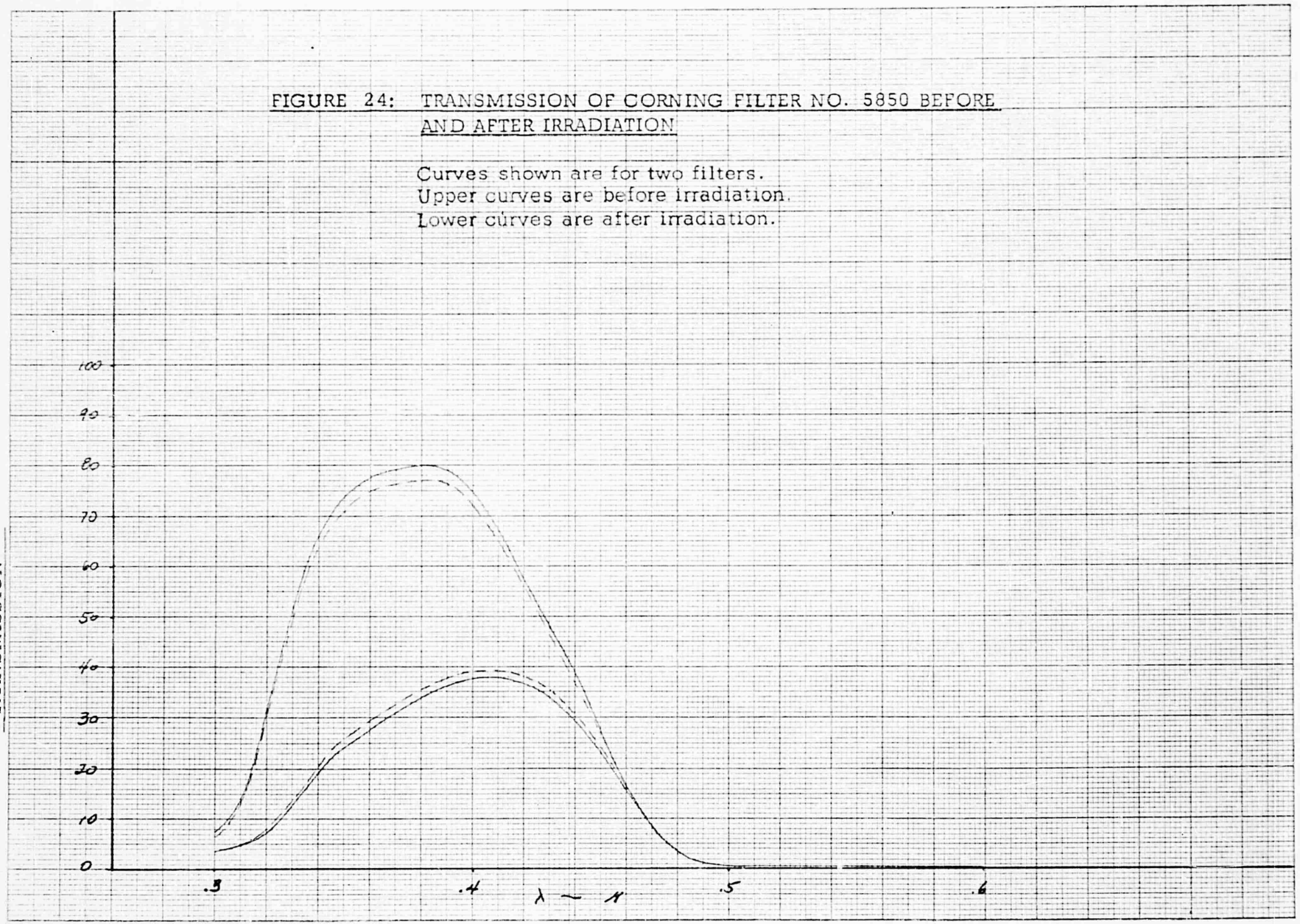

TRANSMISSION

WAVELENGTH (microns)

FIGURE 25: TRANSMISSION OF I.R. ABSORBING FILTER

Upper Curve- Before irradiation.
Center Curve- After 21 hours' irradiation.
Lower Curve- After 84 hours' irradiation.

Filter thickness is .097 inches.

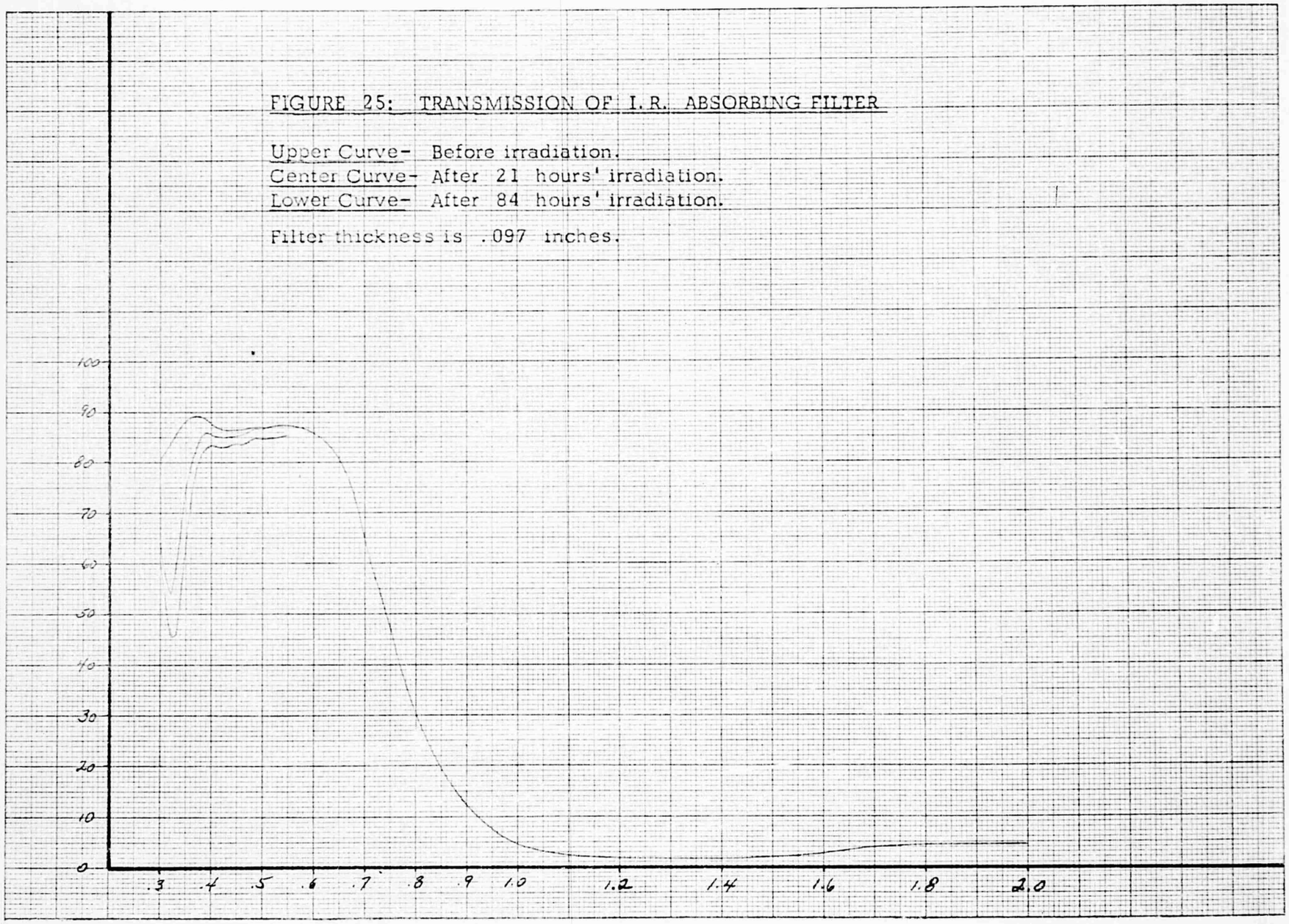

6 Reflectivity and Emissivity Measurements

In carrying out this work reflectance measurements from about 0.3μ to 3μ were essential to be able to calculate an absorptivity for coated and uncoated solar cells. Likewise, reflectance measurements from 5μ to 40μ were essential to calculate the emissivity of the same cells. These values represent the primary criteria for the evaluation of coatings on solar cells. However, the measurement of these values is not a simple and routine procedure even with best apparatus developed today—to the extent that the equipment used in this work had not previously been used to make measurements beyond 15μ. Because of this, numerous problems had to be solved in making these measurements.

6.1 Apparatus and Limitations

A Perkin-Elmer Model 13-U, double beam, single-pass spectrophotometer was used as the basic measuring equipment. Fused silica, sodium chloride, and cesium iodide prisms permitted spectral measurements to be made in the range from 0.2 to more than 40 microns. Detectors used to cover this wide spectral range included a photomultiplier tube, a lead sulfide cell, and a high-sensitivity thermocouple with a cesium iodide window to permit measurements in the far infrared.

Two attachments have been used in conjunction with the spectrophotometer to make spectral reflectance measurements. A Perkin-Elmer Model 205 reflectance equipment enabled measurements to be made from about 1 to 40μ. In this equipment a water-cooled sample is placed in a "black body" cavity held at a temperature of

750° to 1000°C. Radiation from the walls of the cavity is incident on the sample from all directions; rays reflected in one direction nearly normal to the sample surface are directed into the spectrophotometer. This sample beam is compared with a reference beam which also originates within the cavity. This equipment is identical in operation to that developed by Dunkle and Gier.[9]

A Coblentz Hemispherical Reflectometer* was used to make relative reflectance measurements from about 0.3 to 1μ, using an end-on photomultiplier detector. In this equipment, also described in Ref. 9, a monochromatic beam is directed through an opening in an internally silvered hemispherical mirror. This beam is focussed on a sample which is just offset from the center of the hemisphere. Rays reflected in all directions including specular rays are reflected again from the silvered surface of the hemisphere and brought to an approximate focus at a point conjugate to the sample. An end-on photomultiplier tube was used as a detector at this point.

An emissivity apparatus was also obtained from Perkin-Elmer. This apparatus consists of a furnace and sample mount for heating samples to 300° to 600°C. Radiation emitted normal to the surface of the sample can be observed together with a reference beam from the nickel cavity of the reflectance furnace, so that normal spectral emissivity curves can be obtained directly.

A number of difficulties have been experienced in the operation of these equipments, and a number of limitations encountered. These are discussed below, together with experimental results obtained.

---

* This reflectometer was kindly loaned by the U.S. Army Engineer Research and Development Laboratories, Ft. Belvoir, Va., for use in this work.

Spectrophotometer Operation

Several problems were encountered in operation of the spectrophotometer due to working in extended spectral ranges and to using unconventional arrangements in some cases. A high sensitivity thermocouple with a cesium iodide window** was used throughout the work. The output of this thermocouple was two to three times greater than the standard instrument thermocouple in the range of 1 to 15μ. This extended the possible operating range of the instrument using the black body reflectometer source. With this detector and the sodium chloride prism it was found possible to operate in the visible range to about 0.5μ as long as high resolution was not required. This saved considerable operating time by avoiding changing to a lead sulfide detector and fused silica prism. However, it was found essential to use a glass filter at the monochromator entrance slit to avoid considerable scattered light errors when working in the visible and near infrared. Various runs were made to compare results in this range using the lead sulfide and the thermocouple detectors, and the sodium chloride and fused silica prisms. The results were found to generally agree to within 2%.* Likewise the overlap with the photomultiplier detector at 0.5 to 0.6μ generally showed agreement within 2%.

Serious scattered light errors of up to 25% were found using the CsI prism from 15μ to 40μ without appropriate filters. Using an Eastman Kodak No. 245 far infrared filter at the monochromator entrance decreases scattered light to less than 1% from 15μ to 20μ, increasing to about 5% at 23μ. Using a 4-mil black polyethylene filter plus a CaF_2 scatter plate decreases scattered light to less than 1% at 23.5μ, increasing to 3% at 35μ and 10% at 43μ.

---

* All percentage errors given in this section are the difference between two percentage values.

** Purchased from the Charles M. Reeder Co., 171 Victor Ave., Detroit, Michigan.

Model 205 Reflectometer Operation

This equipment consists essentially of a thick wall, heated, cylindrical nickel cavity about 4 inches in diameter and 6 inches high designed to approximate a black body. A water-cooled sample is inserted so as to be flush with the surface of the top of the cavity, and to make an angle of about 15^{o} with a line going through the center of the bottom of the cavity. Two exit beams emerge from an opening in the bottom of the cavity and are used as sources for the double-beam spectrophotometer. One beam originates at the sample, and consists of rays reflected by the sample surface from the surrounding black body. The second beam originates from the cavity roof and is intended to be black body radiation at the same temperature as that seen by the sample. The analysis and design of this equipment has been described in the literature.[10]

During initial operation of this equipment, it was found necessary to modify the sample holder supplied in order to eliminate sporadic water leaks that developed, and that usually damaged the reflecting surfaces on the initial transfer optics. It was also found that the water-cooled sample holder, in contact with the roof of the nickel cavity, cooled the roof an estimated 30 to $40^{o}C$ below the temperature of the cavity sides. An extension was therefore added to the sample holder which raised the lowermost contact of the sample holder to a point two inches above the cavity roof, and which reduced the temperature difference to a few degrees.

Initial reflectance runs on vacuum deposited aluminum mirrors gave good agreement with the published reflectance in the range from 1 to 15 microns. However, as the range of measurement was extended with the cesium iodide prism it was found that the

observed reflectance exceeded 100% at about 17μ, and apparent reflectances of more than 200% were observed in the range of 20 to 25μ. Similar results were also observed at about the same time by J. Maclay, using identical equipment at the Jet Propulsion Laboratory of the California Institute of Technology.

This difficulty was traced to the fact that the nickel cavity is a very poor approximation to a black body in this spectral range. This is shown in Fig. 26, in which the energy radiated from three points on the furnace roof is compared with the energy reflected by a specular aluminum mirror. These data were obtained using the spectrophotometer in single-beam operation, using the same optical path for all measurements, and using fixed slit and gain settings for each wavelength drum setting. If the nickel cavity was in fact a black body all of the curves would be straight lines very nearly superimposed on the aluminum mirror reference line.

It should be noted that Fig. 26 shows the most uniform energy distribution achieved with this equipment. The details of these curves are very sensitive to the alignment of the transfer optics and to positioning of the sample. By not using optimum conditions considerable errors can be introduced into the 1 to 15μ region, and beam energies varying by a factor of 4 have been observed in the 20 to 25μ region. Further, simply rotating the sample holder also introduces large variations as the sample looks at a different portion of the cavity. The shape of the energy curves has been found to vary with the temperature of the cavity.

A possible explanation of these results is that the three beams from the roof of the cavity all see the opening in the bottom of the cavity after only a single reflection from the side wall. This does not happen for the specular mirror sample, since this looks at the side wall of the cavity near the junction of the bottom of

FIGURE 26: RELATIVE ENERGY RADIATED FROM SEVERAL POINTS IN THE BLACK BODY REFLECTOMETER CAVITY

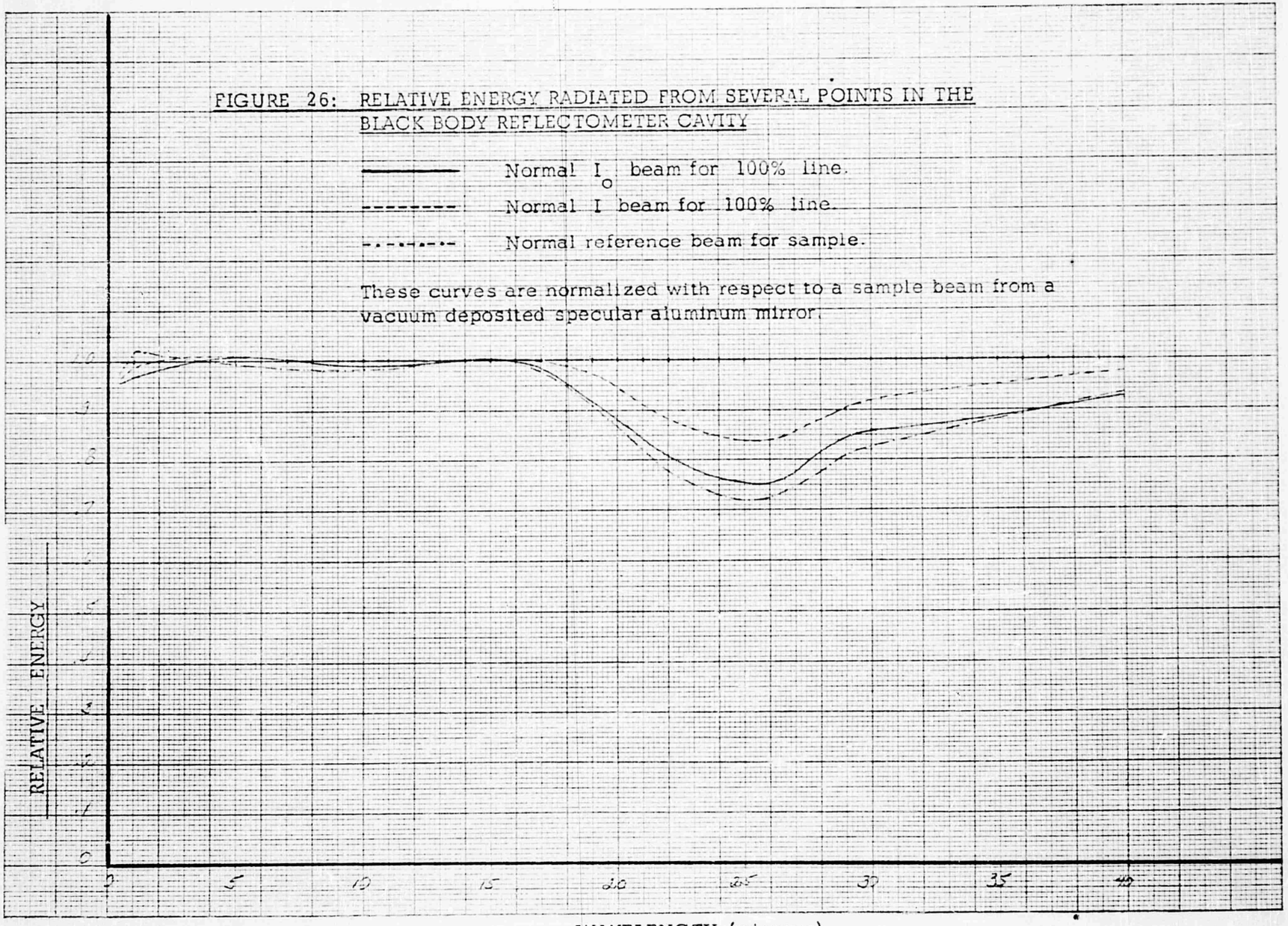

the cavity with succeeding reflections to the top of the cavity.

These results show that it is not possible to measure the absolute reflectance of a sample beyond 15μ using double-beam operation. All runs made in this spectral region were therefore done by recording first the apparent reflectance of a vacuum deposited, specular aluminum mirror, operating double beam, using this as a 100% line. The unknown sample was then placed in the cavity in an identical position and orientation, and the apparent reflectance run double beam. Data from the sample run was then reduced using the aluminum mirror run as a 100% standard. In this way it was possible to use double-beam operation. Data obtained in this way will be correct if the reflectance of the aluminum mirror is 100%, if the mirror and sample are mounted in identical positions, and if the sample is also a specular reflector. Recalling that this procedure is used at wavelengths greater than 15μ, all three of these requirements are considered to be valid within the accuracy of the equipment. It has been found that the reflectance curve of an aluminum mirror coincides with a normal 100% line within 1 to 2% from 15 to about 17μ using the cesium iodide prism. Excellent agreement with published curves for the reflectance of aluminum has also been found below 15μ using the sodium chloride prism.

Another problem encountered in working with this equipment is that the nickel oxide coating frequently chips off of large areas of the cavity interior when the cavity is cooled. The interior of the cavity has been cleaned on several occasions by grit blasting, sand blasting, and chipping off of the oxide by tumbling. The cavity was then re-oxidized using slow heating cycles to 750^{o} and 1000^{o}C. In each case severe chipping of the oxide occurred on trying to cool the furnace to 250^{o}C. to try to make direct

emissivity measurements. These measurements are not possible until this problem can be overcome.

In order to make a comparison of results obtained using different equipments, several samples run at the Hoffman Science Center were submitted to J. Maclay at the Jet Propulsion Laboratory. The black body reflectometer used for this work at J. P. L. was designed and fabricated there, and differs in design details from the Perkin-Elmer unit. This unit appears to be an improved black body approximation in the range of 17 to 25μ. The results obtained on a 12% solar cell-cover glass combination are shown in Fig. 27. This figure also includes data measured by Dunkle [9] several years ago on a 9% solar cell-cover glass combination. From 1μ to 15μ the three curves agree with maximum differences in reflectance of about 6%, while the H. S. C. and J P L. curves agree within 2 to 3% over most of this range. Beyond 15μ differences as large as 10% occur, which can not be readily explained. In this range the H. S. C. curve was obtained using a cesium iodide prism, the other two curves using potassium bromide prisms. Scattered light errors, difference in prism dispersion, and decreasing transmission of potassium bromide beyond 20μ could contribute to these differences, but these differences should be minor. The difference more likely arises from the radiation characteristics of the "black body" cavities.

In terms of the desired end result, namely the total emissivity, the difference between the H. S. C. and the J. P. L. curves from 15.5 to 24μ is not large. The value of 0.83_3 from the H. S. C. curve is increased by 2% to 0.85_0 on substituting the J. P. L. results in this range.

Similar differences have been found between H. S. C. and J. P. L. curves for silicone coated cells and for cells with U. V. reflecting cover glasses, as shown in Fig. 28.

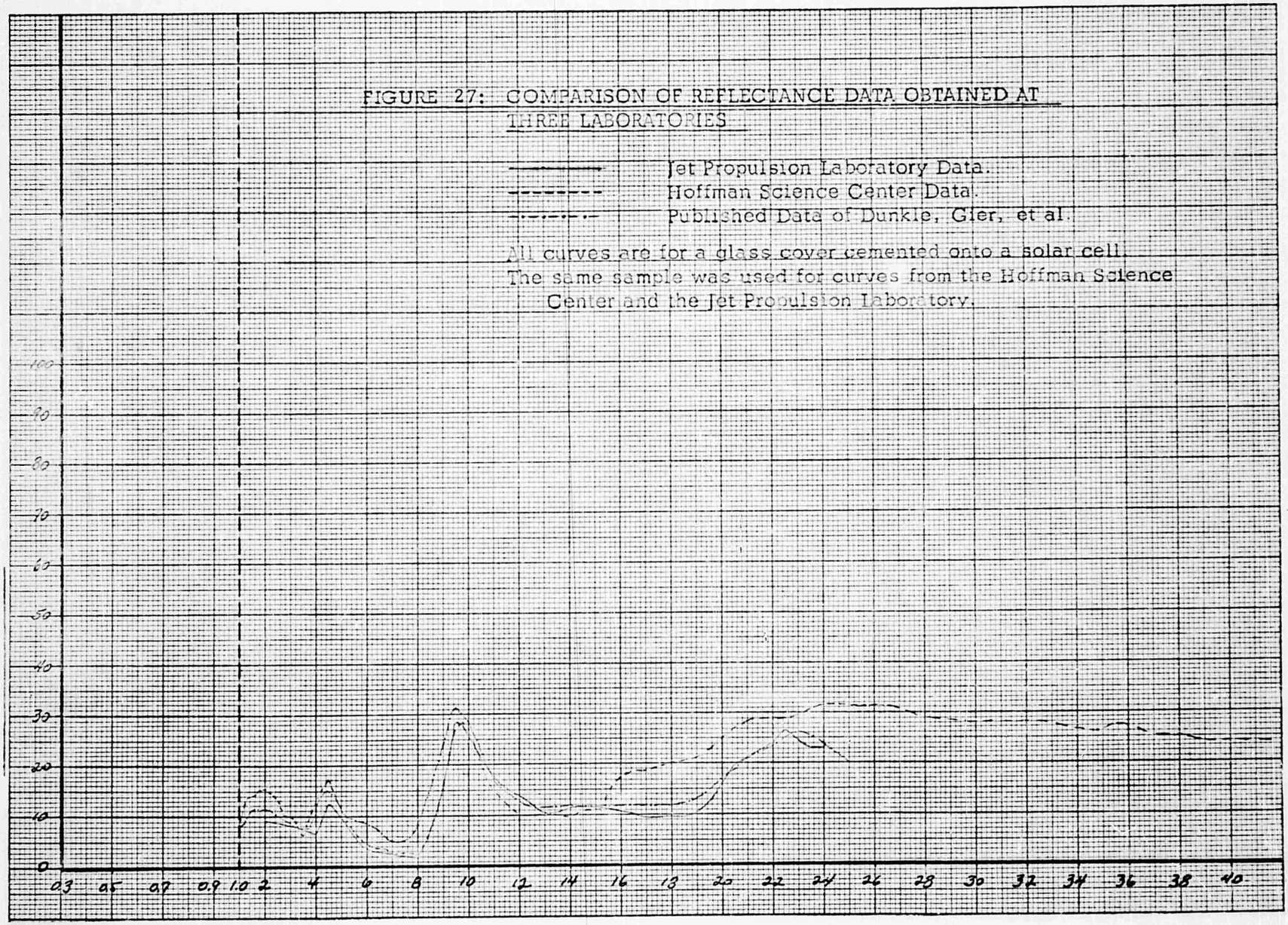

FIGURE 27: COMPARISON OF REFLECTANCE DATA OBTAINED AT THREE LABORATORIES

——————— Jet Propulsion Laboratory Data.
- - - - - - - - Hoffman Science Center Data.
-·-·-·-·- Published Data of Dunkle, Gier, et al.

All curves are for a glass cover cemented onto a solar cell. The same sample was used for curves from the Hoffman Science Center and the Jet Propulsion Laboratory.

FIGURE 28: COMPARISON OF REFLECTANCE DATA

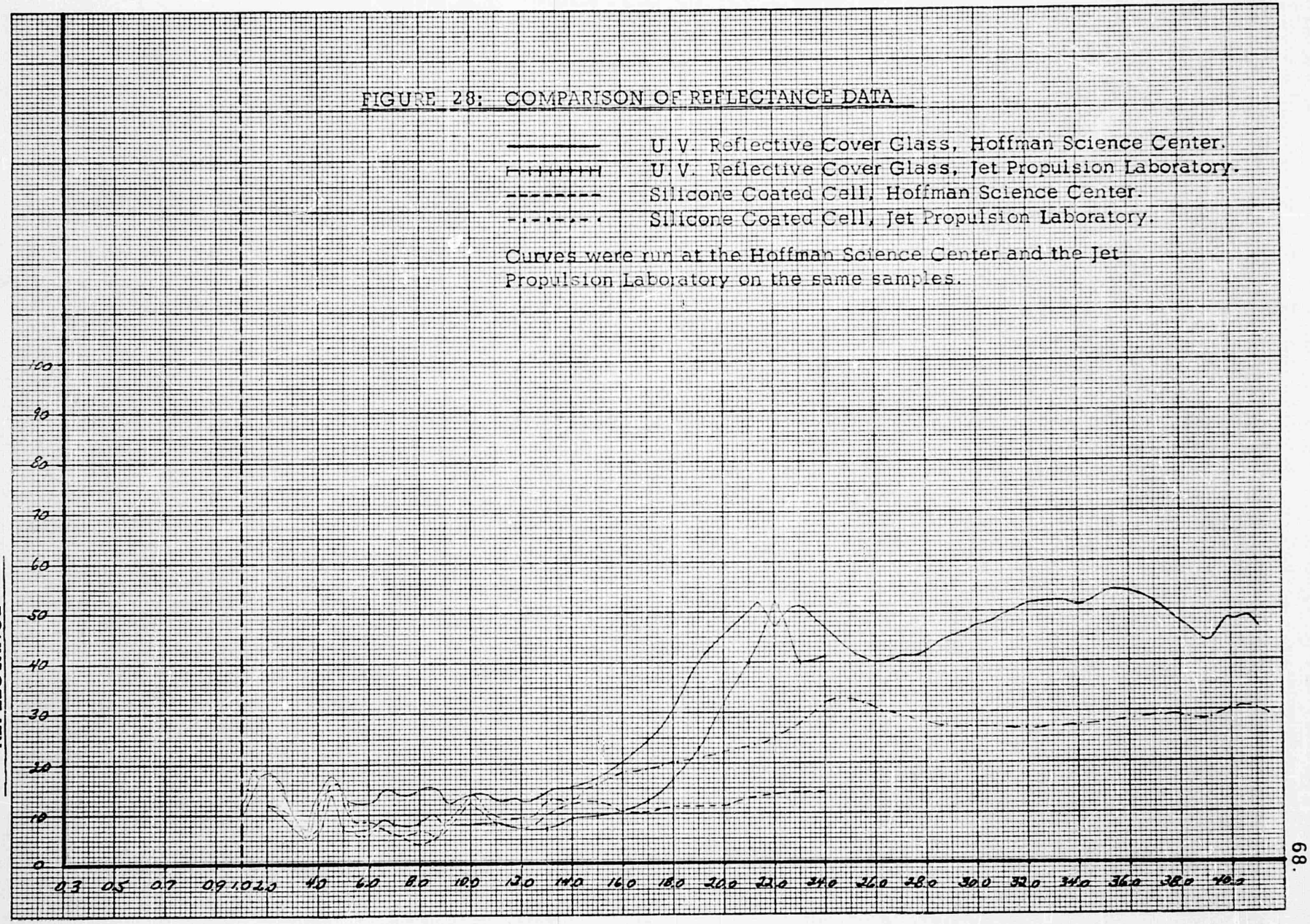

Reflectances measured with this equipment include the normal specular reflectance plus the normal component of the diffuse reflectance of the sample. (Although the reflected rays observed make an angle of 75^{o} with the surface of the sample, these are considered to be normal rays for purposes of this discussion.) At longer wavelengths the dimensions of the surface roughness of the solar cell surface are less than the wavelength of the radiation and the cell becomes a specular reflector. Therefore at these wavelengths only the normal specular reflectance is measured. It is important to note that in no case is the total integrated reflectance measured, as is required to calculate the total emissivity using Kirchoff's law. The emissivity values calculated from the reflectance data measured here are approximations to the normal emissivity [3, 11]

Coblentz Hemisphere

As mentioned previously this equipment can only be used to make relative measurements, in which the reflectance of an unknown sample is compared with a reference standard. This equipment was originally designed and used to make measurements in the infrared using a Golay detector. For the present work an end-on photomultiplier detector was substituted, since the equipment can in principle be used equally well in the visible and ultraviolet spectral regions. The photomultiplier used, an R.C.A. No. C7297 with an S-5 response, was connected directly into the power supply and recorder circuits of the spectrophotometer. The reflectometer proper was mounted, with appropriate transfer optics, so that the exit slit of the monochromator was focussed on the sample. The sample holder was modified to permit alternate viewing of three samples, each being mounted at an

angle of 15^{o} to the incident beam, as in the black body reflectometer.

All runs were made using both a specular aluminum mirror and an aluminized solar cell as reference standards. All mirrors used in this work, as well as with the black body reflectometer, were specially prepared to obtain coatings of maximum reflectivity.[12] These were vacuum deposited onto substrates cleaned by glow discharge bombardment, at pressures in the 10^{-5} mm. range, using very rapid deposition rates. Deposition times required were approximately 2 seconds. Polished glass substrates were used for all specular mirrors.

During the initial runs made with this equipment it was found that the relative reflectance of samples changed greatly as the voltage applied to the photomultiplier was varied from 450 to 800 volts. It was found possible to eliminate this voltage dependence with the use of a diffusing coating of magnesium oxide smoke about 1 mm. thick deposited onto the end of the photomultiplier.

A major problem in attempting to use this equipment was in the selection of reference standards to be used. This problem was made more difficult by the fact that the coated cells tend to be specular reflectors and the uncoated cells diffuse reflectors.

In an effort to duplicate the angular dependence of reflection for solar cells, aluminum was vacuum deposited on cells as well as on polished glass substrates, to provide two reference standards.

The observed reflectance of an aluminized, 12% solar cell, with respect to a specular aluminum mirror, is shown in Fig. 29. Additional curves are shown for a 12% solar cell with respect to both the specular mirror and the aluminized cell. No correction has been applied for the reflectivity of aluminum. The minimum in reflectance of the aluminized cell at 0.36μ is characteristic of all cells run, and is not found in specular reflectance curves for vacuum deposited

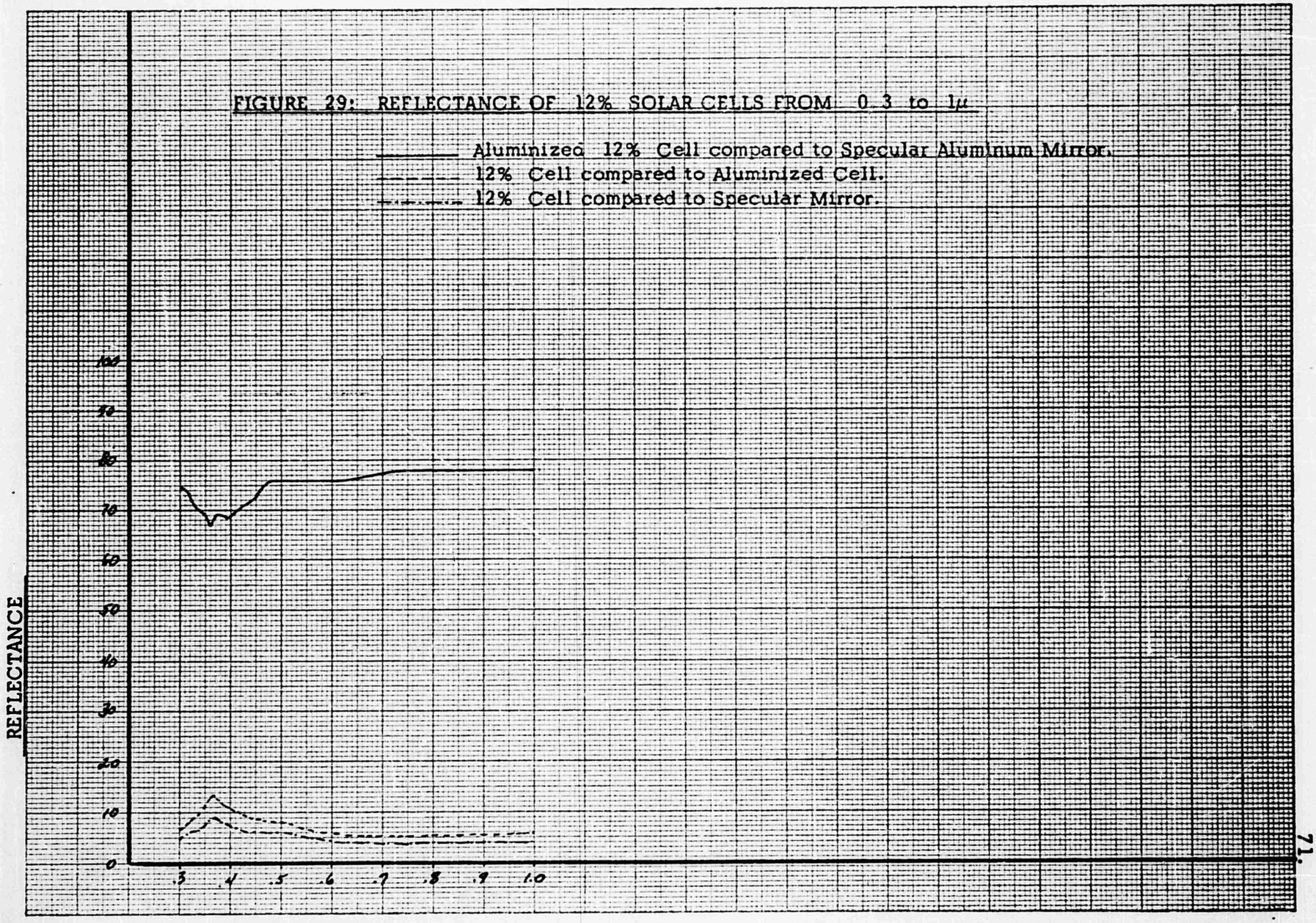
FIGURE 29: REFLECTANCE OF 12% SOLAR CELLS FROM 0.3 to 1μ
Aluminized 12% Cell compared to Specular Aluminum Mirror.
12% Cell compared to Aluminized Cell.
12% Cell compared to Specular Mirror.
REFLECTANCE
100
90
80
70
60
50
40
30
20
10
0
.3
.4
.5
.6
.7
.8
.9
1.0
WAVELENGTH (microns)

aluminum given by Hass.[12] This may result from the deposition of the aluminum at angles other than normal to the surface, which is known to affect the appearance of aluminum deposits. However, the two reflectivity curves for the 12% solar cells agree within 1% to 4% from 0.3 to 1μ. These two curves can be considered as limits for the reflectance of the cells.

For comparison, Fig. 30 shows results obtained for a silicone coated cell using the Coblentz hemisphere, as compared with results on a similar sample obtained using an integrating sphere.[13] It can be seen that spectral reflectance values from the latter curve are very nearly midway between the two curves obtained using the hemisphere.

Reflectance curves used subsequently for calculations of absorptivity have been taken as the average of the curves obtained using the two reference standards, except in the case of the U.V. reflective cover glass where the specular reflectivity of the sample required a specular mirror reference. These curves are shown in Fig. 31.

6.2 Experimental Results

Reflectance curves from 0.3 to 1.1μ are given in Fig. 31 for several Hoffman 120 CG, 12% gridded cells. Results are given for a bare cell and for cells coated with silicone, with a cover glass and with a U.V. reflective cover glass. These data were measured using the Coblentz Hemisphere, and are the data used for subsequent calculations of absorbance.

Typical reflectance curves are shown in Figs. 32 and 33 for a similar group of cells from 1μ to about 40μ. All the data in Fig. 32 were obtained in March, 1961. The data from 1μ to 15μ in Fig. 33 were obtained in February, 1961; those from 15μ to 40μ

FIGURE 30: REFLECTANCE OF SILICONE COATED CELL, 0.3 — 3.39μ

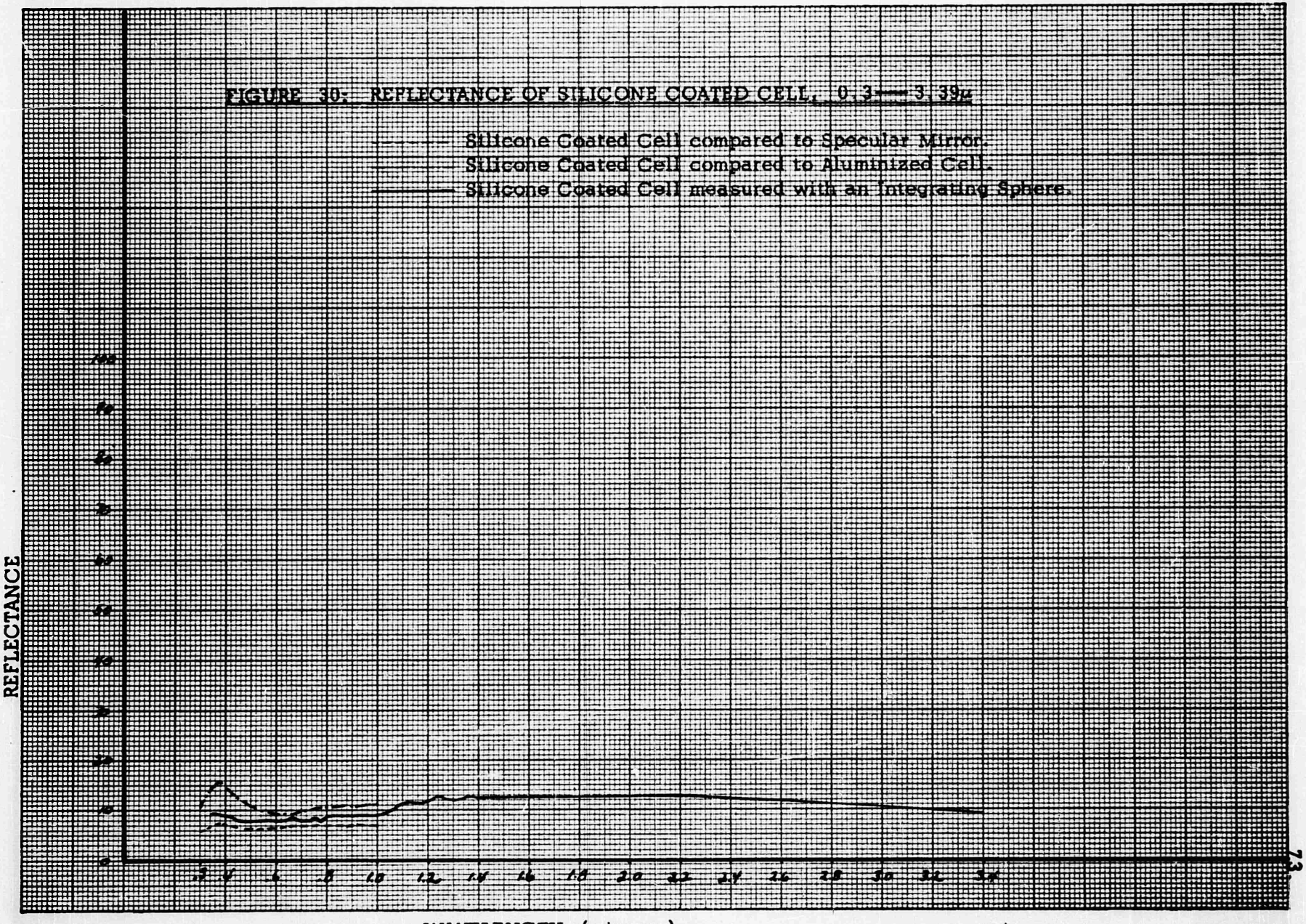

FIGURE 31: SPECTRAL REFLECTANCE OF SOLAR CELLS FROM 0.3 to 1.1μ

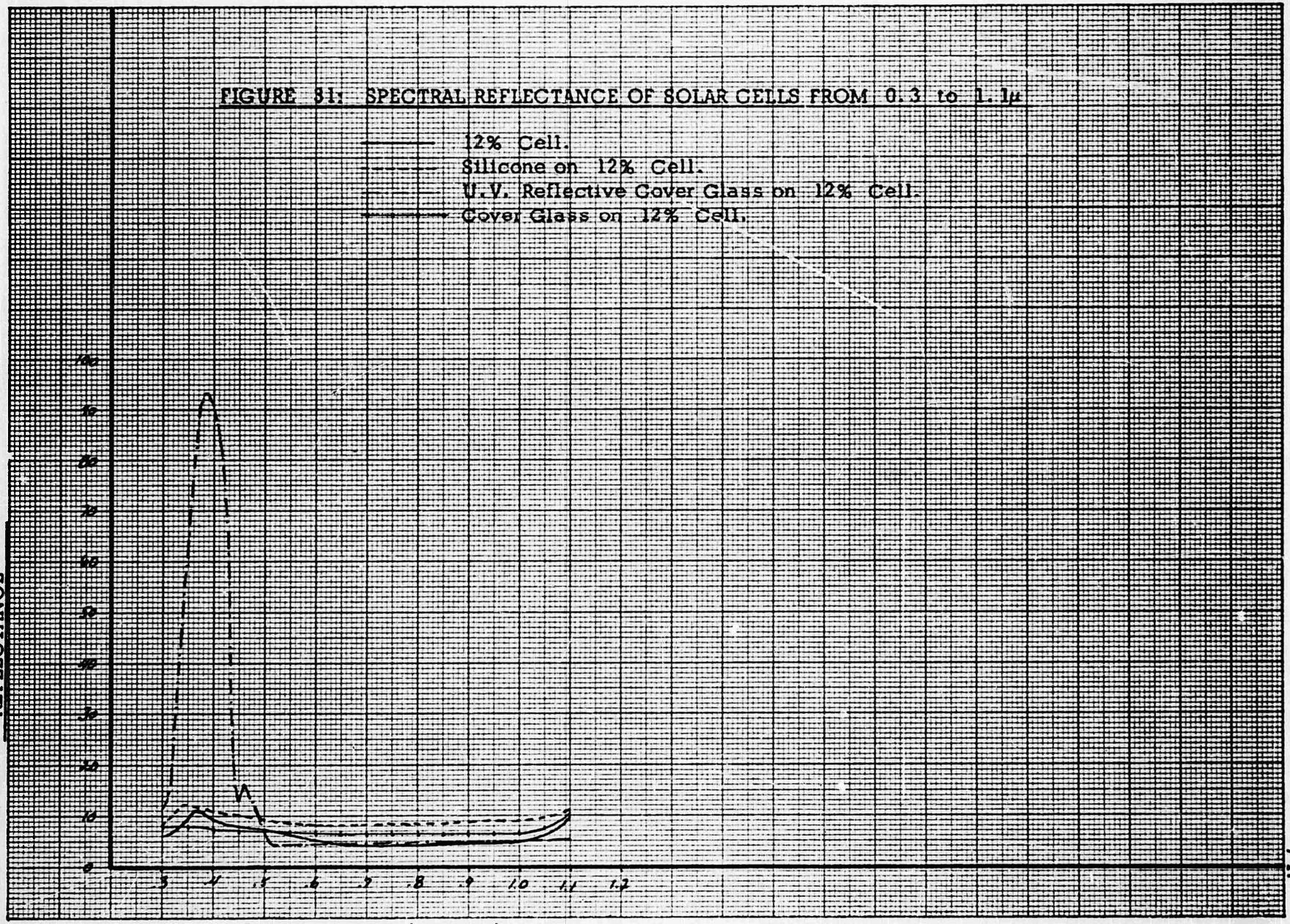

FIGURE 32: SPECTRAL REFLECTANCE OF SOLAR CELLS FROM 1μ TO 38μ

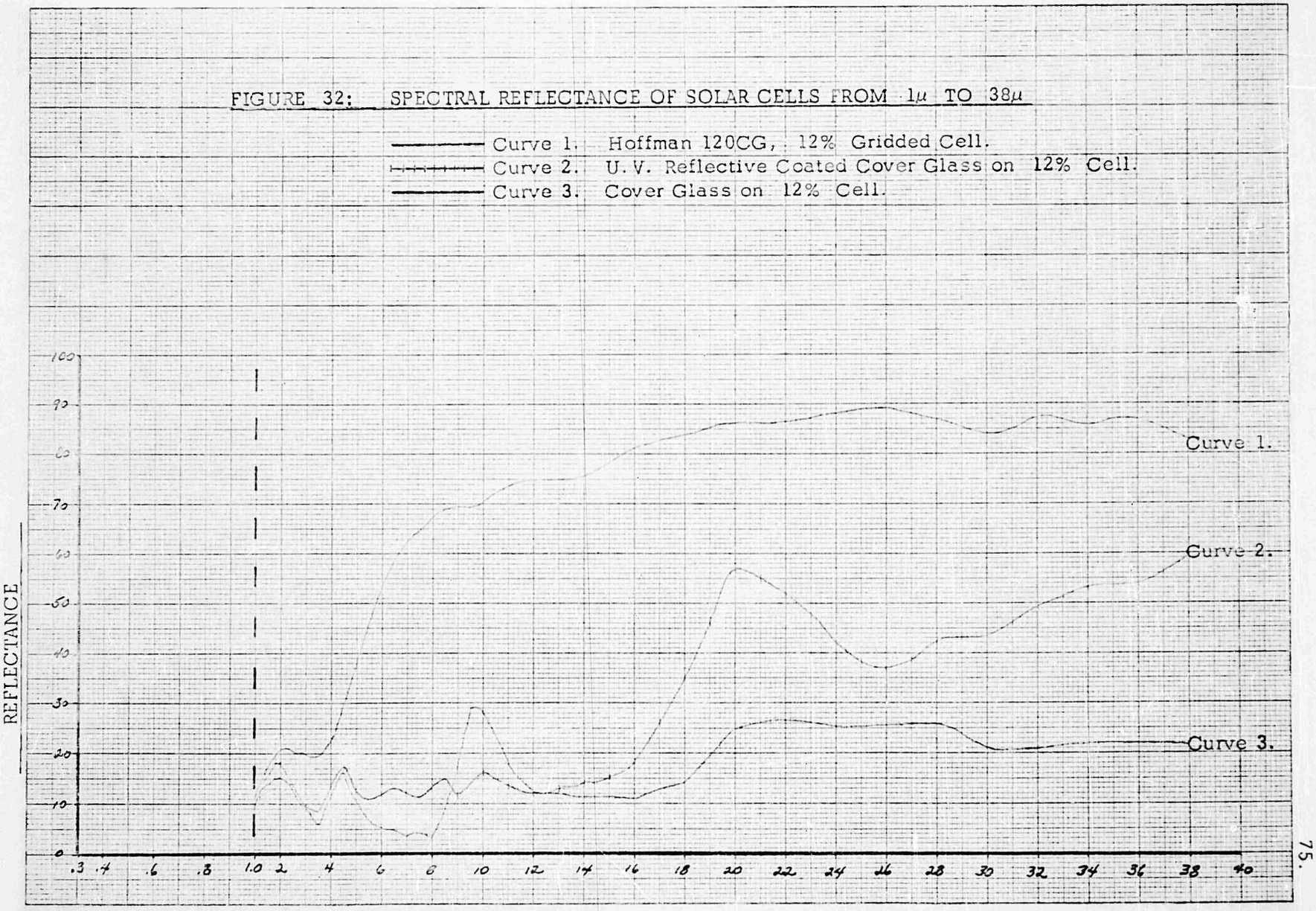

FIGURE 33: SPECTRAL REFLECTANCE OF SOLAR CELLS FROM 1μ TO 42μ

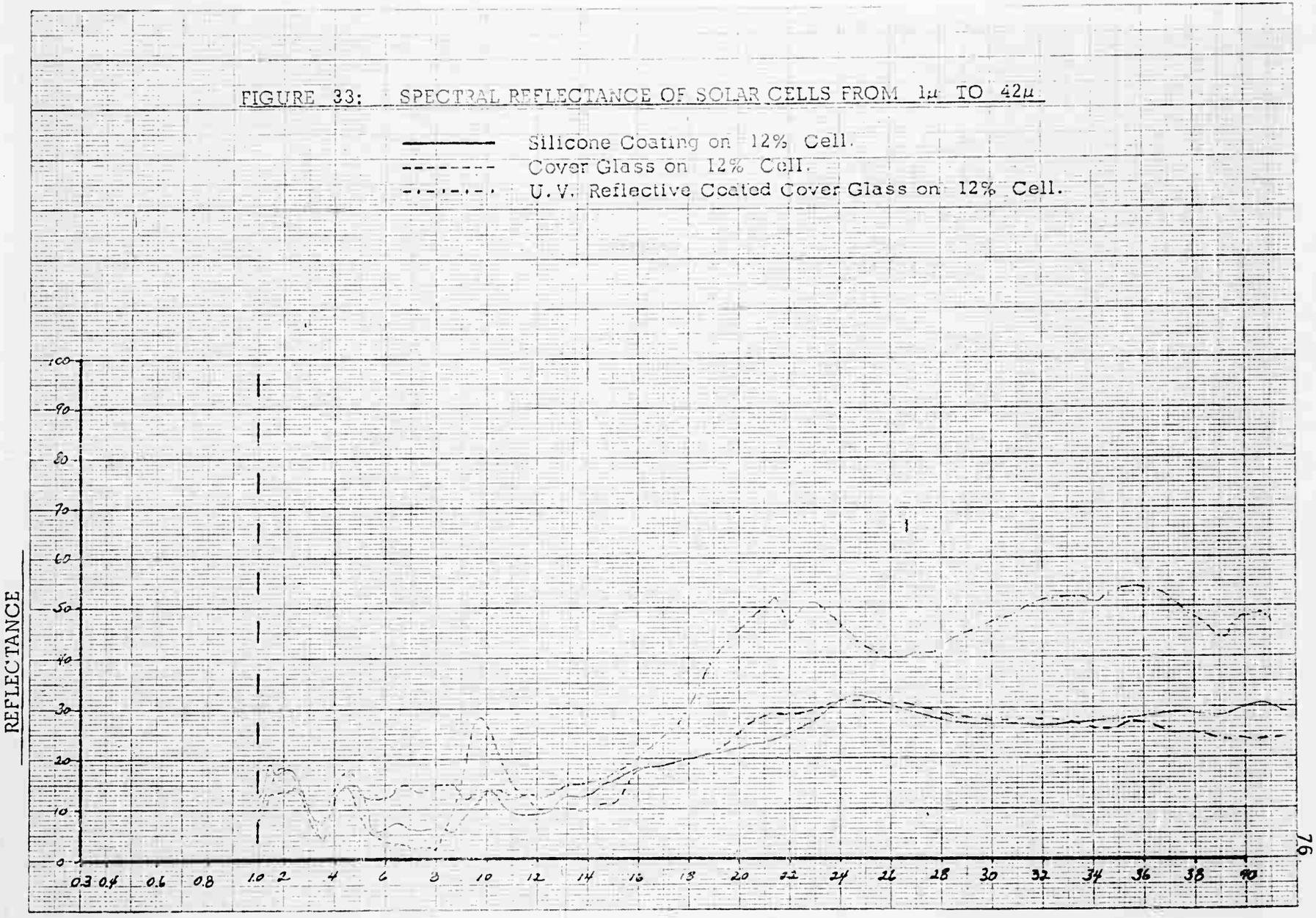

in December, 1960. Comparing the two curves for the cover glass and for the U.V. reflective cover glass on cells, it can be seen that these agree within 5% for most wavelengths. A comparison of the effect of these differences on calculated emissivities is given below.

6.3 Emissivity and Absorptivity Calculations

Emissivities have been calculated graphically, by plotting the point-by-point product of the reflectance curve and a black body radiation curve. Areas under the curves are then measured using a planimeter, and the area ratios computed. As an example, the curves used in reducing the data from Fig. 33 are shown in Fig. 34. Emissivities which have been calculated using reflectance data from both Fig. 32 and Fig. 33 are given in Table V.

Total absorptivity values have been calculated similarly, using the solar spectral distribution curve shown in Fig. 1 and reflectance data from Figs. 31 to 33. These are also given in Table V.

The same reflectivity data used to calculate absorptivity can also be combined with spectral response data, shown in Fig. 4, to calculate the relative electrical output of coated cells. These results are also given in Table V.

The data in Fig. 33 show that the emissivity of the silicone coated cell exceeds that of the cover glass on a cell only because of the reflectance peak at 9.7μ which is characteristic of all silicate glasses. This wavelength corresponds to about the maximum in the black body radiation curve for $50^{\circ}C$.

The difference between the two cover glasses is particularly interesting because it shows the considerable effect even a very thin coating can have on the emissivity of the substrate.

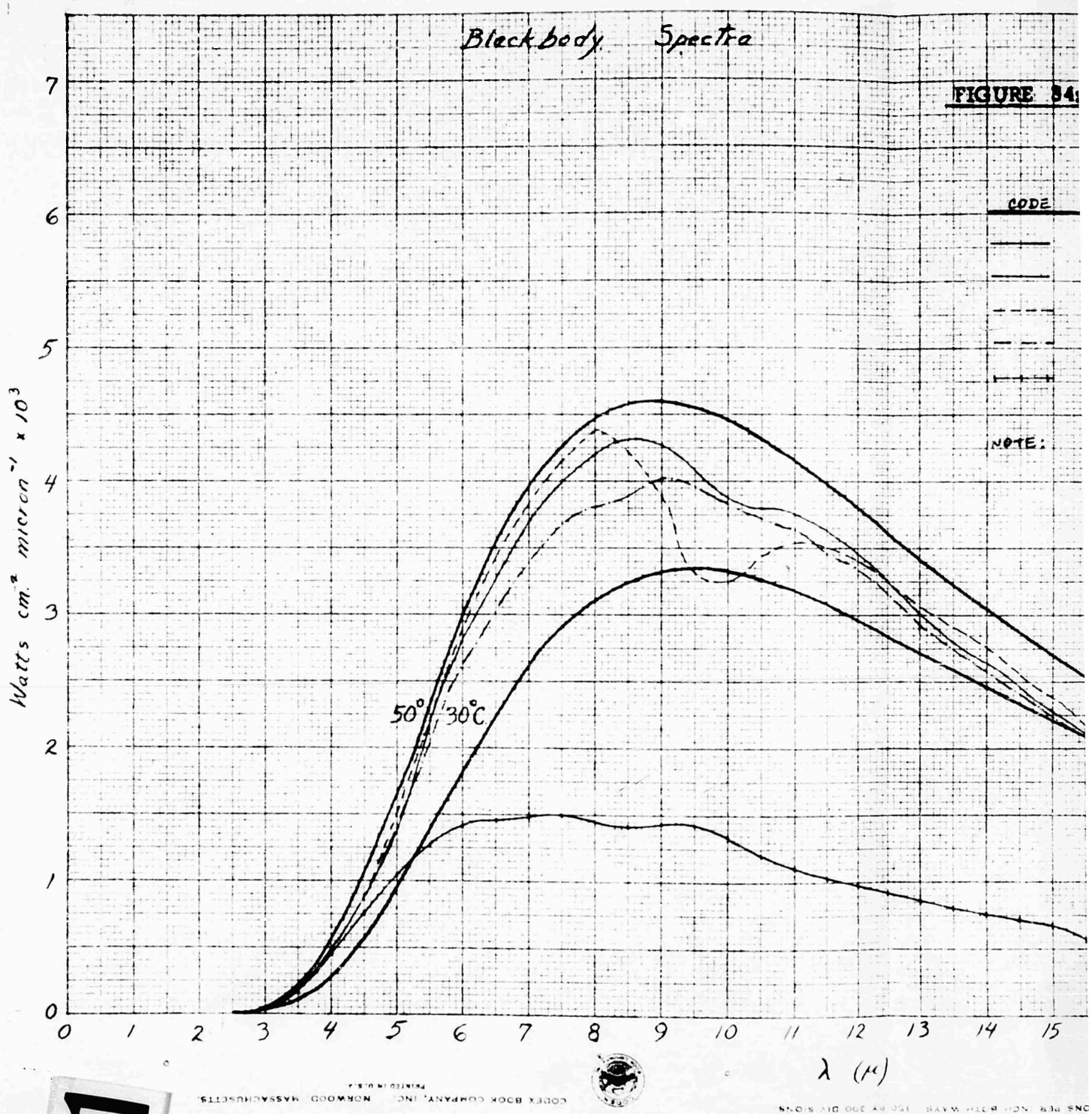
Blackbody Spectra
FIGURE 84
CODE
NOTE:
Watts cm.⁻² micron⁻¹ x 10³
0
1
2
3
4
5
6
7
0
1
2
3
4
5
6
7
8
9
10
11
12
13
14
15
λ (μ)
50°
30°C

FIGURE 84: EMISSIVITY CALCULATION FOR COATED SOLAR CELLS

CODE	SAMPLE	AREA	EMISSIVITY AT 50°C
———	BLACK BODY SPECTRA AT 50°C	29.93 in²	
———	SILICONE ON CELL 140A	25.30 in²	0.846
- - - -	UNCOATED COVER GLASS ON CELL	24.92 in²	0.832
— — —	COATED COVER GLASS ON CELL	23.20 in²	0.776
— · — · —	UNCOATED 12% GRIDDED CELL	7.91 in²	0.264

NOTE: ALL CELLS ARE HOFFMAN 120CG, 12% GRIDDED CELLS

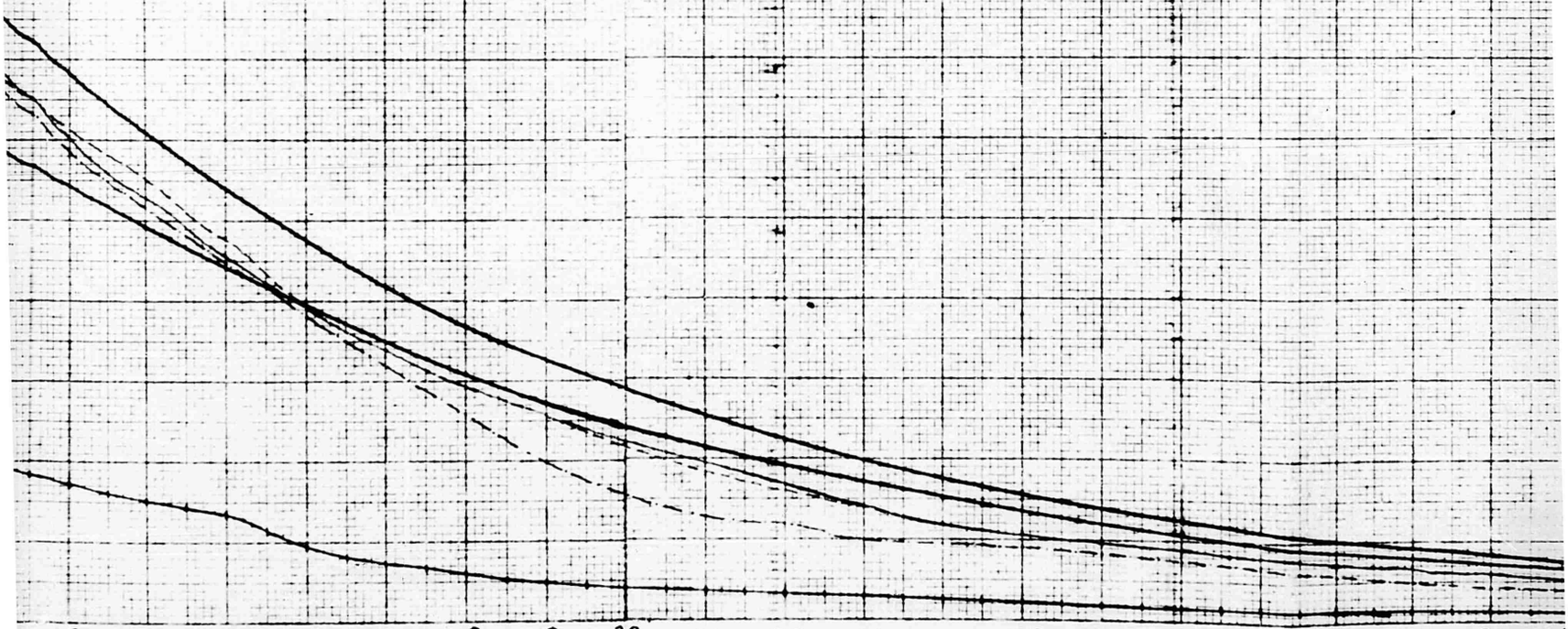

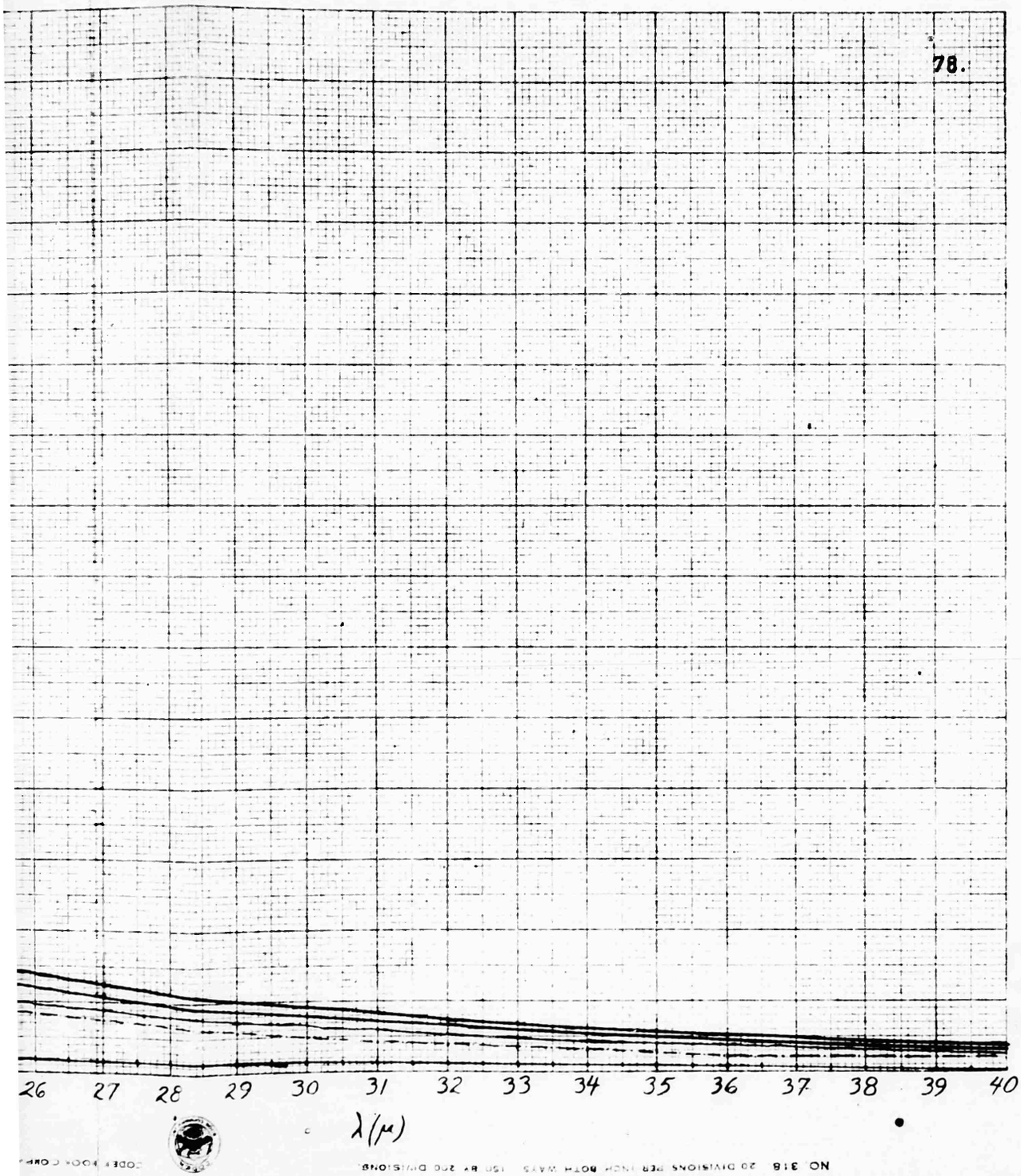

3

TABLE V: EMISSIVITY AND SOLAR ABSORPTIVITY OF COATED SOLAR CELLS

	Emissivity at 50°C		Absorptivity	Relative Cell Output
	(a)	(b)	(c)	(d)
12% Solar Cell	0.26_4	-----	0.90_2	1.00
Silicone Coating on Cell	-----	0.84_6	0.87_6 (e)	0.95_7
Cover Glass on Cell	0.85_3	0.83_2	0.90_1	0.98_3
U.V. Reflective Cover Glass on Cell	0.77_7	0.77_6	0.84_7	0.96_7

(a) Calculated using data from Fig. 32.

(b) Calculated using data from Fig. 33.

(c) Calculated using data from Figs. 31-33.

(d) Calculated using data from Figs. 4 and 31.

(e) The absorptivity calculated for a silicone coated cell, using reflectance data from Jet Propulsion Laboratory shown in Fig. 30, is 0.89_0.

Two vacuum deposited coatings prepared elsewhere were evaluated. One of these was a coating supplied by the Bausch and Lomb Optical Co., Rochester, New York, which was developed specifically as a high emissivity, vacuum deposited coating. The reflectance of this coating is shown in Fig. 35. By comparison with similar curves for silicone coatings and glass covers, it can be seen that the Bausch and Lomb vacuum deposited coating has an appreciably lower emissivity. In addition, six cells to which this coating was applied showed an average decrease in short circuit current of 11.8%. No further consideration was given to this coating.

Several cells were also coated by the Optical Coating Laboratory, Santa Rosa, California. A 29-layer selective infrared reflecting coating was deposited directly onto several cells, and onto several silicone coated cells. The objective was to learn if a reflective interference coating might be used in conjunction with a high emissivity coating, and it was planned to apply a silicone coating over the infrared reflective coating. After deposition of the coating it was found that all cells appeared to have been grossly overheated. This was exhibited by the condition of the solder electrodes, and by considerable cracking of the silicone coatings. It was estimated that the cell temperatures had to be $300^{\circ}C$ or more to account for these results. Therefore, this approach is not possible unless ways can be developed to keep the cell temperature to a maximum of $150^{\circ}C$. It should be noted, however, that no outgassing problem was encountered during the coating deposition, which is an excellent indication of the stability of the silicone under these extreme conditions.

FIGURE 35: REFLECTIVITY OF BAUSCH & LOMB AND OPTICAL COATING LABORATORY COATINGS

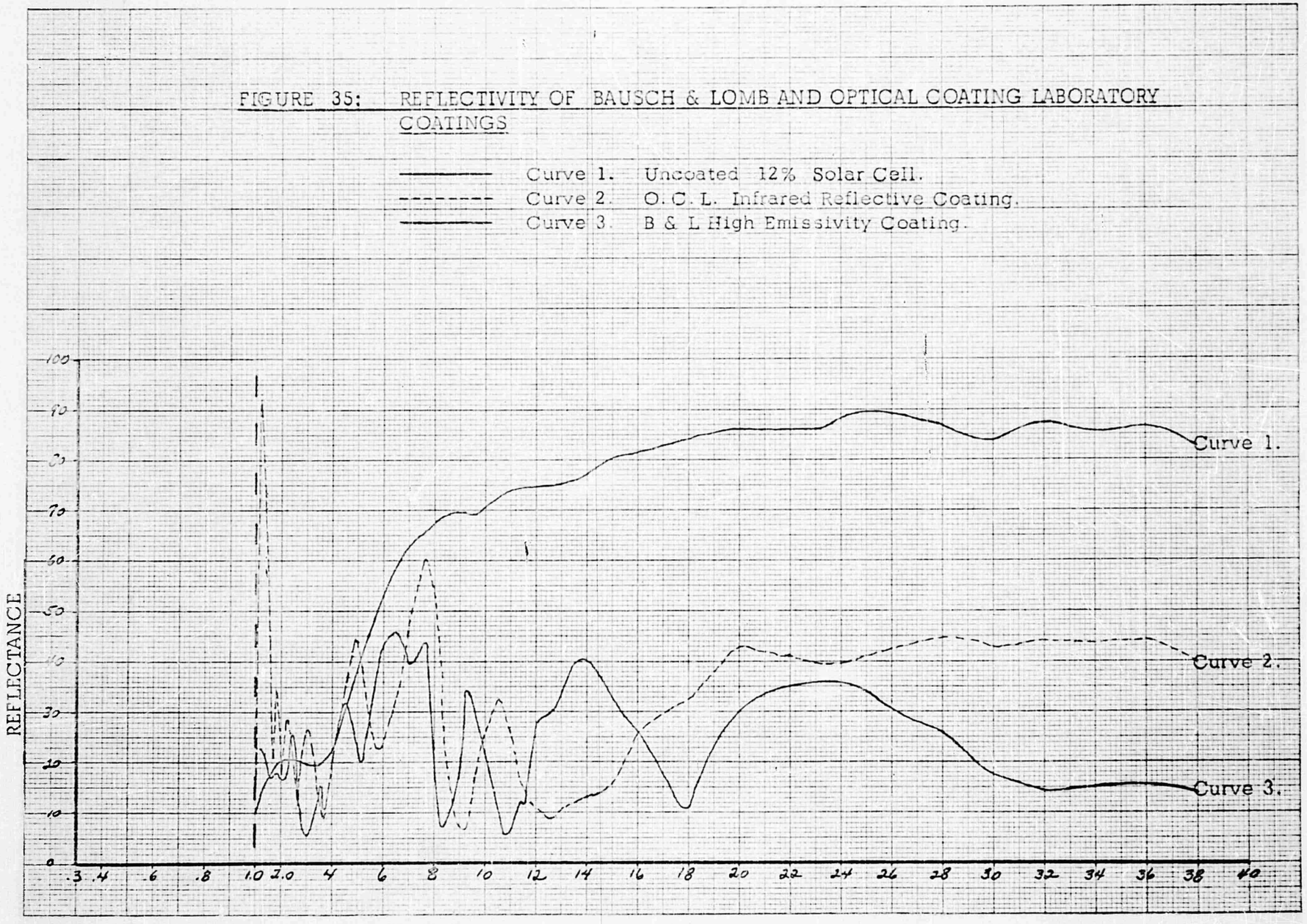

7 Evaluation of Silicone Coated Test Panels in Sunlight on Table Mountain

Two test panels were obtained to evaluate the effect of silicone coatings using Jet Propulsion Laboratory test facilities at Table Mountain. Each panel consisted of four shingles, each with five solar cells of nominal 13% efficiency. The panels were fabricated using materials and techniques identical to those used on panels for Ranger flights.

Panel 1 was spray coated with a 2.8-mil layer of XR 6-2044 silicone and cured 3 hours at 150°. The current-voltage curves for both panels were then measured in a series of runs at Table Mountain, in which direct solar radiation, sky radiation, and panel temperature were monitored and recorded. A silicone coating was then applied to Panel 2, and the current-voltage curves of both panels run again. The maximum power output was then determined for each run, and these values were standardized to a total incident radiation intensity of 0.110 watts/cm^2-min. From data among the runs, in which temperature varied from 9.3 to 25.0°C., a temperature dependence of maximum power output of 0.00291 watts/°C. was calculated. The variation in maximum power with temperature is known to be nearly linear in this temperature range.[2] Using this value, all power outputs were standardized to 10°C. The results are shown in Table VI.

The results from Panel 1 show that the maximum power observed in March was 0.044 watts, less than the values found in the three runs during February. This result can arise from a different spectral distribution of incident radiation, which in turn can arise from changing sky radiation and other atmospheric effects. The total radiant energy on the cell is the sum of the direct solar radiation plus

TABLE VI: MAXIMUM POWER OUTPUT OF UNCOATED AND SILICONE COATED SOLAR CELL TEST PANELS

Date	Approx. Sky Radiation	Panel 1- After Coating	Panel 2- Before Coating	Panel 3- After Coating
21 February 1961	0%	0.977 watts	1.027 watts	---
23 February 1961	3.7%	0.977 watts	1.026 watts	---
23 February 1961	3.5%	0.978 watts	---	---
9 March 1961	10%	0.934 watts	---	0.935 watts

Each value is the average of five (5) runs for February data, and four (4) runs for March data. Each series of runs was completed within 11 minutes.

sky radiation. The sky radiation is measured by the change in output of a silicon solar cell when exposed to direct sunlight only and when exposed to total sun and sky radiation. The correction required for sky radiation in the March readings was about 10%, as compared with zero to 3.7% for all other readings.

If the March reading for Panel 2 after coating is increased by 4.7%, the difference found for Panel 1 between the February and the March results, the maximum power output of Panel 2 is 1.026 watts before coating and 0.979 watts after coating. This is a decrease in maximum power output of 4.6% as a result of applying the coating.

The measured decrease in maximum power output of 4.6% as a result of applying a silicone coating is comparable to an average decrease of about 5% which has been found on applying U.V. reflective glass covers on cells.[14]

8 Energy Balance in Space. Comparison of Coatings.

The efficiency of conversion of solar energy to electricity in space is a function of the spectral response of the cell as modified by its coating, and the total absorptivity and emissivity of the cells and their backing. The spectral response of an uncoated cell has been shown in Fig. 4, and the calculated relative power output of cells with the several coatings considered given in Table V. If an uncoated cell is assumed to have a conversion efficiency of 9% in space at a particular temperature, the efficiencies of the coated cells are: silicone coating, 8.61%; cover glass, 8.85%; and U.V. reflective cover glass, 8.70%.

In space the conversion efficiency is modified by the operating temperature, which must be calculated from the cell conversion efficiency, total solar absorptivity, the emissivity of the cell and the emissivity of the cell backing.

The data used and the calculated temperatures and efficiencies are given in Table VII.

A comparison can be made between the relative output of an uncoated cell and a silicone coated cell as calculated from optical measurements, and as measured directly in sunlight on Table Mountain. The relative cell outputs in Table V were calculated from spectral reflectance curves, the spectral response of a solar cell, and the spectral distribution of sunlight in space. These results show that application of a silicone coating decreases the maximum power output of a cell by 4.3%. Direct measurements on Table Mountain of an uncoated and a silicone coated panel showed a decrease of 4.6%. These values agree remarkably well. Since a difference in cell output is being compared, the results of the Table Mountain test should not change significantly if these were run in space.

TABLE VII : EFFICIENCY AND OPERATING TEMPERATURE OF COATED SOLAR CELLS IN SPACE

	Cell efficiency[a]	Total solar absorptivity	Emissivity of cell at 50°C[b]	First Approximation		Second Approximation	
				Operating temperature °C	Cell efficiency	Operating temperature °C	Cell efficiency
Uncoated Cell	9.00	.902	.264	90	6.39	93	6.25
Silicone Coating on Cell	8.61	.876	.846	52	7.66	53	7.62
Cover Glass on Cell	8.85	.901	.832	56	7.73	57	7.23
U.V. Reflective Cover Glass on Cell	8.70	.847	.776	52	7.76	53	7.67

(a) A conversion efficiency of 9% at 30°C in space is assumed for an uncoated cell.

(b) Emissivity of 0.887 is assumed for back surface of cell.

REFERENCES

1) F. S. Johnson: J. Meterol. 11 431-9 (1954).

2) M. B. Prince and M. Wolf: Brit. Inst. Radio Engrs. 18, No. 10, 583-95 (1958).

3) M. Jakob, "Heat Transfer," pp. 41-43, John Wiley & Sons, New York, 1949.

4) F. A. Jenkins and H. W. White, "Fundamentals of Optics," pp. 523-526, McGraw-Hill Book Co., New York, 1957.

5) J. F. Hall, Jr.: J. Opt. Soc. Amer. 50 717-20 (1960).

6) F. M. Noonan, A. L. Alexander, and J. E. Cowling, "The Properties of Paints as Affected by Ultraviolet Radiation in Vacuum - Part I," Naval Research Laboratory Report 5503, July 13, 1960.

7) A. Charlesby, "Atomic Radiation and Polymers," Pergamon Press, New York, 1960.

8) R. C. Hirt, R. G. Schmitt, N. D. Searle and A. P. Sullivan: J. Opt. Soc. Amer. 50 706-13 (1960).

9) R. V. Dunkle: First Symposium on Surface Effects on Spacecraft Materials, "Spectral Reflectance Measurements," pp. 117-137, John Wiley & Sons, New York, 1960.

10) J. T. Gier, R. V. Dunkle and J. T. Bevans: J. Opt. Soc. Amer. 44 558 (1954).

11) R. M. Witucki and A. E. Lewis, "Integral Coatings for Solar Cells-Third Quarterly Report," p. 37, July 15-October 15, 1960.

12) G. Hass: J. Opt. Soc. Amer. 45 945-952 (1955).

13) Private communication, W. Schaefle, Jet Propulsion Laboratory, Pasadena, California.

14) Private communication, M. Wolf.